REVIEW

Nanomaterials for Engineering Stem Cell Responses

*Punyavee Keratitayanan, James K. Carrow, and Akhilesh K. Gaharwar**

Recent progress in nanotechnology has stimulated the development of multifunctional biomaterials for tissue engineering applications. Synergistic interactions between nanomaterials and stem cell engineering offer numerous possibilities to address some of the daunting challenges in regenerative medicine, such as controlling trigger differentiation, immune reactions, limited supply of stem cells, and engineering complex tissue structures. Specifically, the interactions between stem cells and their microenvironment play key roles in controlling stem cell fate, which underlines therapeutic success. However, the interactions between nanomaterials and stem cells are not well understood, and the effects of the nanomaterials shape, surface morphology, and chemical functionality on cellular processes need critical evaluation. In this Review, focus is put on recent development in nanomaterial–stem cell interactions, with specific emphasis on their application in regenerative medicine. Further, the emerging technologies based on nanomaterials developed over the past decade for stem cell engineering are reviewed, as well as the potential applications of these nanomaterials in tissue regeneration, stem cell isolation, and drug/gene delivery. It is anticipated that the enhanced understanding of nanomaterial–stem cell interactions will facilitate improved biomaterial design for a range of biomedical and biotechnological applications.

1. Introduction

Advances in nanotechnology have resulted in the development of advanced biomaterials with custom property combinations. A range of biomedical nanomaterials have been developed to mimic tissue complexity and modulating stem cell functions, resulting in many therapeutic benefits.[1] In this Review, we focus on nanomaterials that possess at least one physical dimension between 1–100 nm utilized in tissue engineering. Nanomaterials are not a simple miniaturization of macroscopic counterparts; they exhibit distinctive physical, chemical, optical, and mechanical properties due to a high specific surface area.[2–4] The unique properties of nanomaterials offer implementation in nanoelectronic devices to biomedical applications.[4–7] The applications of nanomaterials in biomedical research emanate from similar length scales with the majority of biological moieties such as structural protein, deoxyribonucleic acid (DNA), signaling molecules, antibodies, and extracellular matrices (ECMs). A cell itself is essentially a multifunctional particle comprised of nano compartments such as cell membranes, surface proteins, cytoskeletons, and nuclear membranes containing DNA. Owing to their small size, nanomaterials can widely interact with the physiological environment and enable the development of systems that mimic structural complexity and functions of ECMs.[7,8] For example, an ECM is a dynamic structure that consists of different nanofibers (such as collagen, actin filaments, etc.), nanocrystals, and signaling molecules. Because nanomaterials are small enough to interact and alter cellular-level functions, they are expected to provide a new framework for medical intervention and diagnosis.

Stem cells are unspecialized precursor cells with self-renewal capacity and the potential to differentiate into different lineages given the appropriate signals.[9] Stem cells can be classified into two types: embryonic stem cells (ESCs) obtained from the inner cell mass of the blastocyst, and adult stem cells, found in postnatal tissues such as the umbilical cord, bone m arrow, dental pulp, adipose, and neuron tissues.[10] ESCs are an ideal cell source for regenerative medicine due to their indefinite self-renewal and pluripotency. However, there are some ethical questions concerning the use of embryos to obtain ESCs. Multipotent adult stem cells are an alternative with fewer ethical issues, but they have limited differentiation and self-renewal capacity, limiting their applications.[11,12] Hence, researchers have attempted to reprogram somatic cells into pluripotent stem cells by somatic cell nuclear transfer (SCNT) and by inducing the expression of embryonic transcription factors to generate induced pluripotent stem cells (iPSCs). Still, the reprogramming efficiency and the epigenetic abnormalities of the cells differentiated from SCNT and iPS cells are debatable.[13] Because of the confluence of nanomaterials and stem cells, the restoration and regeneration of diseased cells and tissues are becoming a clinical possibility that will result in therapies for currently incurable diseases.

However, certain challenges must be addressed before stem cells can be fully applied to medical treatments. These include controlling self-renewal processes, proliferation, and regulating the differentiation of stem cells.[14,15] Nanomaterials have the ability to control stem cell behavior due to their small size

P. Keratitayanan, J. K. Carrow, Prof. A. K. Gaharwar
Department of Biomedical Engineering
Texas A&M University
College Station, TX 77843, USA
E-mail: gaharwar@tamu.edu
Prof. A. K. Gaharwar
Department of Materials Science and Engineering
Texas A&M University
College Station, TX 77843, USA

DOI: 10.1002/adhm.201500272

and bioactive characteristics.[14–17] Research has shown that chemical composition, surface topography, mechanical characteristics, electrical properties, and morphological properties of nanomaterials significantly influence stem cell responses.[14–19] For example, ceramic nanoparticles such as synthetic silicates induce osteogenic differentiation of adult stem cells without using any growth factors.[20] In other studies, quantum dots, fluorescent carbon nanotubes, and magnetic nanoparticles were used for labeling stem cells, permitting a noninvasive monitoring after transplantation, and subsequent delivery of drugs and genes into stem cells.[6,16,21,22] Sjöström et al. reported that the height of pillar-like nanostructures on a titanium scaffold greatly influenced mesenchymal stem cells behaviors.[23] Specifically, the stem cells on the 15 nm high pillars were spread with a large focal adhesion, whereas those on the 100 nm high pillars formed a small focal adhesion with poorly defined cytoskeletons.[23] All these studies showed that nanomaterials can be designed to provide an inductive microenvironment to direct stem cell differentiation in a controllable manner. Overall, a range of multifunctional nanomaterials for tissue engineering applications have been developed and investigated over the past few years. However, the interactions between nanomaterials and stem cells are not completely understood.

In this Review, we critically evaluate the interactions between different types of nanomaterials with stem cells, focusing exclusively on tissue engineering applications. Stem cells employ a host of biological mechanisms to respond to incorporated nanomaterials, dependent on material type, structure, chemical functionality, and topographical characteristics. These cellular responses provide tissue engineers with a host of tools to control stem cell behavior and achieve a targeted therapeutic outcome, like tissue regeneration, cancer treatment, or immune modulation. First, we discuss the effect of nanotopography, such as nanofibers and nanopatterns, in controlling stem cell behavior. Second, we critically evaluate interactions between stem cells and different nanomaterials. A range of nanoparticles, including polymeric, ceramic, carbon-based, and metal/metal oxide nanomaterials to control stem cells' adhesion, proliferation, and differentiation. Finally, we discuss some of the emerging trends in the field of nanomaterials for stem cell engineering (**Figure 1**). It is expected that the enhanced understanding of nanomaterial–stem cell interactions will be beneficial in designing the next generation of clinical therapies.

2. Nanotopography for Stem Cell Engineering

ECMs provide crucial information to regulate stem cell behavior and tissue formation. For example, a cardiac ECM is composed of a nanoscale interweave pattern of elastin and collagen fibrils that form a dense network with ECM molecules, which forces cardiomyocytes to couple mechanically to one another, forming elongated bundles of anisotropic syncytium.[24] One of the approaches to direct the stem cell fate is to provide physical clues that allow the cells to sense the clue and direct their fate (**Figure 2**). Stem cells have been shown to sense and differentially respond to substrate nanotopography. The phenomenon of mechanotransduction profoundly affects their morphology, proliferation, gene expression, and, ultimately, differentiation.[24,25] For example, stem cell behavior could be dictated solely by altering nanotopography.[26] Several engineering techniques have been developed to obtain structures with nano features, including nanofibrous scaffolds and nanotopographical surfaces.[27,28] Nanofibrous scaffolds fabricated by electrospinning or phase-separation techniques create a biomimetic microenvironment in the length scale that cells normally encounter within their extracellular milieu. These fibrous scaffolds possess a large surface-area-to-volume ratio with highly interconnected porosity to modulate cell migration.[29,30] Similarly, nanopatterning provides control over the degree of cell adhesion, spreading, and migration. In this section, we discuss two major strategies—nanofibrous structures and nanopatterning—to control stem cell behavior.

Akhilesh K. Gaharwar is directing the Inspired Nanomaterials and Tissue Engineering Laboratory in the Department of Biomedical Engineering at Texas A&M University, USA. He received his Ph.D. in Biomedical Engineering at Purdue University and postdoctoral training at Massachusetts Institute of Technology and Harvard University. His research interest includes nanomaterials, cell-nanomaterials interactions, microfabrication technologies, hydrogels, stem cell biology, and tissue engineering. His current research effort centers on creating bioactive nanomaterials for modulating the behavior of stem cells and understanding underlying nanomaterials induced cell signaling for developing bioengineering strategies for tissue regeneration.

2.1. Stem Cell Interaction with Nanofibrous Structures

By controlling the surface morphology, alignment, and topography of fibrous scaffolds, stem cell fate can be modified to engineer different tissue types (Figure 2a). Both electrospinning and phase separation are versatile techniques to fabricate nanofibrous scaffolds from polymer and polymer blends.[27,31,32] A range of physical and chemical properties can be controlled by changing the processing parameters. Additionally, surface modification techniques can also be employed to fine-tune the stem cell fate. A variety of polymers and polymer blends have been used to create nanofibrous scaffolds using electrospinning and phase-separation techniques, such as poly(caprolactone) (PCL), poly(L-Lactic acid) (PLLA), and PLLA/collagen blend.[30,31,33]

Among these polymers, PCL is one of the most widely studied. Xie et al. reported the effects of randomly and uniaxially aligned PCL nanofibers on ESC differentiation into neural lineages.[34] The cells seeded on random nanofibers localized to form embryoid bodies (EBs), while those seeded on aligned nanofibers migrated along the fiber axes and differentiated into mature neuronal lineages. There were fewer astrocytes on

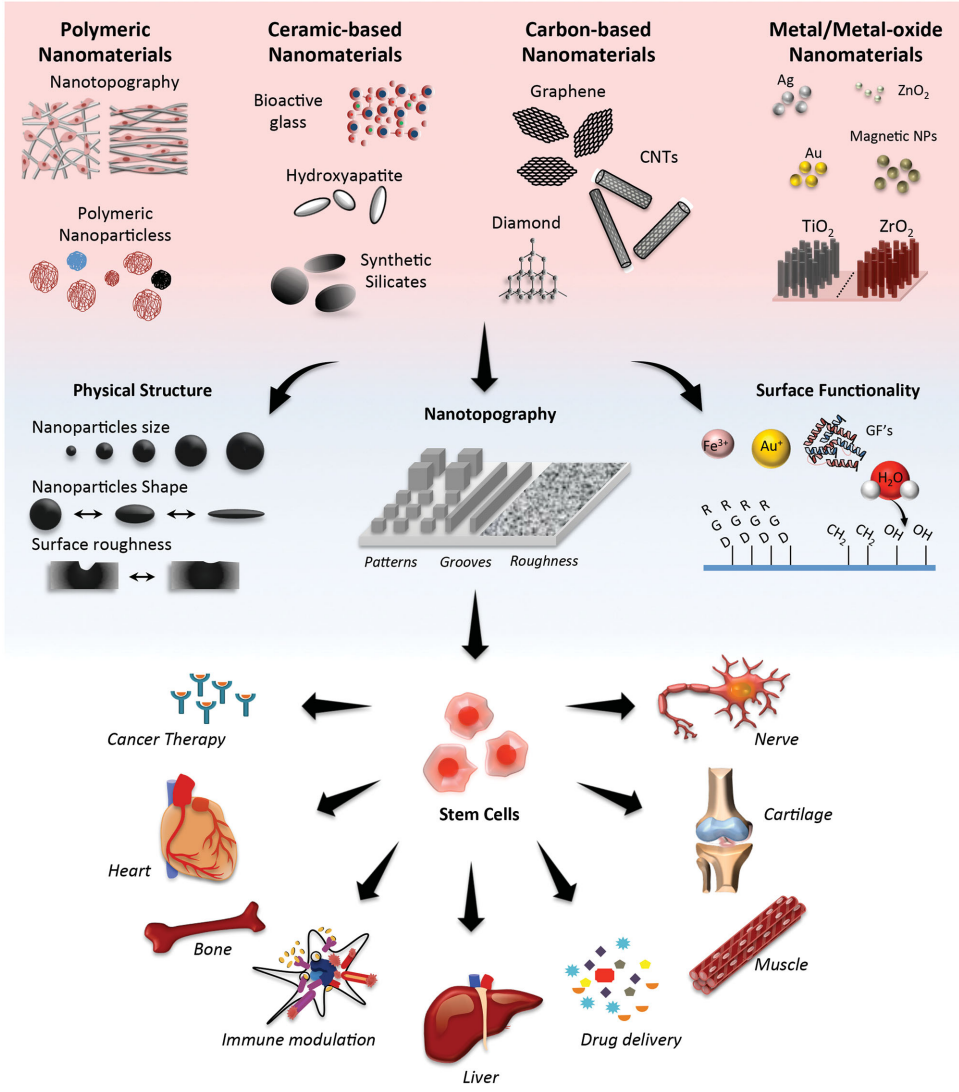

Figure 1. Nanoparticle interactions with stem cells comprise interplay of multiple mechanisms, including physical, chemical, or surface interactions. Physical interactions are dependent on size, shape, and stiffness of the nanoparticles, whereas chemical interactions include the presence of ions, growth factors or hydrophilic moieties. Surface interactions revolve around surface patterning, like nanopillar spacing or size and surface roughness. similarly, chemical modification to the nanomaterial surface via introduction of cell binding sites. The combined effects of these various interactions contribute to the differentiation capabilities of the nanomaterial and can lead to a variety of tissues including but not limited to cardiac, bone, hepatic, muscle, cartilage, and nerve tissues. Some of the emerging applications of nanomaterials include immune modulation and smart drug delivery devices.

aligned nanofibers, which helped in reducing glial scar formation during spinal cord injury.[34] However, the formation of a functional junction between mature neuronal cells needs to be investigated.

Similar studies were conducted with neural stem cells (NSCs) on electrospun PCL. Lim et al. reported that cells on aligned nanofibers elongated and neurites extended along the fiber axes.[35] Consistent with Xie et al., other studies found greater fractions of immature neuronal markers (Tuj1+) on the aligned fibers compared to the random ones.[34,35] The significant number of Tuj1+ cells on aligned fibers was attributed to two mechanisms.[35] First, the aligned fibers promoted the attachment and growth of neuronal progenitors while having a negative selection against non-neuronal cells. Second, the topography changed the cell-fiber contact patterns, leading to cytoskeleton rearrangements and subsequent changes in intracellular canonical Wnt/β catenin signaling, which correlated with increased neurogenesis of NSCs.[35] Further investigation is still needed to identify the transition steps connecting structural changes with downstream signaling pathways.

Electrospun PCL is also used to dictate chondrogenic differentiation for engineering a superficial zone of articular cartilage.[36] In one study, stem cells seeded on nanofibrous scaffolds promoted chondrogenesis compared to those seeded on microfibrous scaffolds,[36] mainly due to the circular morphology of stem cells seeded on nanofibrous scaffolds, versus the elongated cells on microfibrous scaffolds. Cells on nanofibers produced high levels of glycosaminoglycan (GAGs), collagen type II and aggrecan, suggesting that nanofibrous PCL scaffolds may be suitable for regenerating a superficial zone of articular

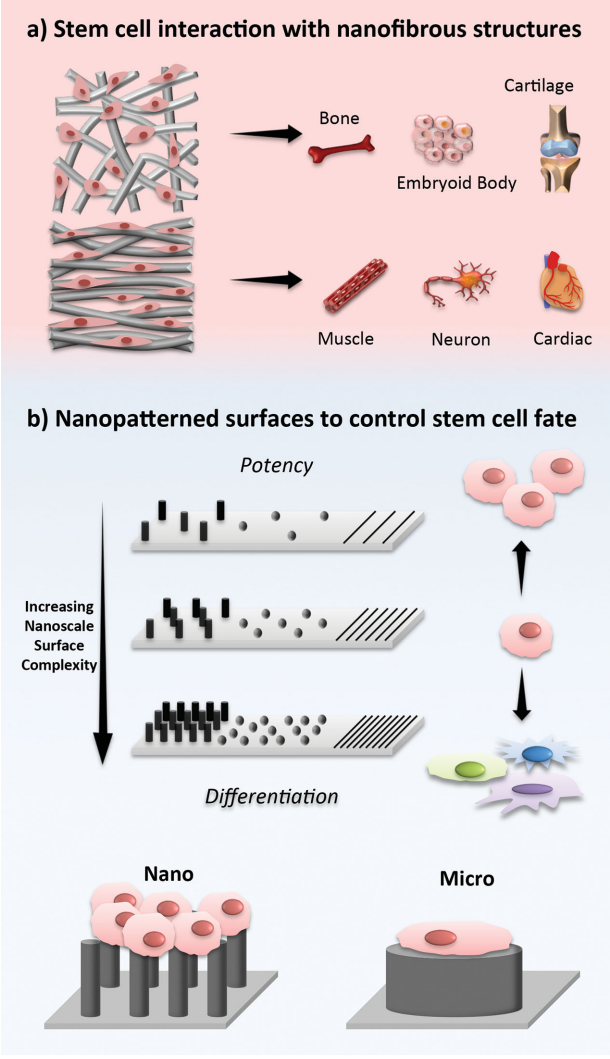

Figure 2. Various nanotopographical modifications alter cell behavior and therefore stem cell outcomes. a) Random nanofibers promote embryoid body, bone, and cartilage formation, while aligned nanofibers show enhanced neuronal induction with directed neurite extension as well as cardiac and myogenic induction. b) Surfaces with increasing nano-complexity and roughness via nanopillars, nanodots, or nanogrooves induce differentiation while smoother surfaces are preferential for potency maintenance. Nanopillars augmented cell adhesion and growth versus micropillars while also forming large cell aggregates, while micropillars induced greater cell spreading.

cartilage, which is naturally enriched with collagen type II.[36] Similarly, Binulal et al. employed electrospun PCL scaffolds for bone tissue engineering and reported that mesenchymal stem cells (MSCs) spread more rapidly and proliferated better on nanofibrous scaffolds compared to microfibrous counterparts.[37] They suggested that the protein conformation on nanofibers might be more favorable for stem cell–material interactions. However, they observed that the protein coverage (proteins per unit fiber surface area) on nanofibers was lower than that on microfibers. The total proteins adsorbed on nanofibers were greater than those adsorbed on microfibers but resulted in lower protein coverage when divided by the significantly higher surface area.[37] It is possible that the number of adsorbed proteins might be more important than the coverage, where not all surfaces of nanofibrous scaffolds are accessible for proteins. Nevertheless, further studies focusing on protein conformations might reveal the underlying mechanisms.

The mechano-topographic modulation of a stem cell's nuclear shape can be used to modulate cell behaviors by intra/extracellular perturbations. In particular, the deformation of nuclear morphology has been correlated with changes in gene expression.[38] Nathan et al. reported that MSCs on aligned PCL nanofibers were elongated and had a higher nuclear aspect ratio (NAR) than cells seeded on random scaffolds.[38] Moreover, the application of static tension has been found to stretch the fibers, subsequently further lengthening the cells and reorienting nuclei in the direction of the applied load. Interestingly, compared with MSCs, fibrochondrocytes (differentiated cells) were reported to be less sensitive to changes in fiber alignment and external forces, perhaps due to different nuclear stiffness, i.e., the intrinsic nuclear stiffness increases with differentiation.[38] Furthermore, stem cells from different sources were found to respond differently to the same nanotopography. Kolambkar et al. showed that amniotic fluid stem cells (AFSCs) on electrospun PCL had a higher initial attachment and proliferation rate when compared to MSCs.[39] Also, in an osteoconductive medium, AFSCs displayed a delayed alkaline phosphatase (ALP) activity but enhanced mineralization. These studies indicate that there might be strong correlation between nuclear shapes and stem cell fate.

Another technique to fabricate nanofibrous scaffolds is phase separation. Smith et al. studied osteogenic differentiation of ESCs on PLLA scaffolds with nanofibrous architecture.[40] Using the phase-separation technique, nanofibers with a diameter similar to that of collagen type I in the bone ECM (50–500 nm) were fabricated. Cells seeded on nanofibrous matrices assumed round-shaped morphology and displayed enhanced interaction with surrounding nanofibers' structure in 3D microenvironments compared to cells on a solid substrate. The enhanced cell-fibrous interaction resulted in upregulation of osteogenic markers. However, one of the drawbacks of these nanofibrous scaffolds was lack of cellular infiltration, which could limit the tissue regeneration since cell penetration is a crucial factor to success in tissue engineering. Use of other fabrication techniques such as porogen leaching along with phase separation might provide scaffolds with micrometer-sized pores for enhanced cellular infiltration.

A range of synthetic polymers can be used to fabricate nanofibrous scaffolds using phase-separation techniques. Xu et al. developed 3D nanofibrous scaffolds via phase-separation techniques using polyhydroxyalkonates (PHA), a family of polyester biopolymers that includes PLA, poly(3-hydroxybutyrate) (PHB), poly(3-hydroxybutyrate-*co*-3-hydroxyvalerate (PHBV), poly(3-hydroxybutyrate-co-3-hydroxyhexanoate) (PHBHHx), and poly(3-hydroxybutyrate-co-4-hydroxybutyrate) (P3HB4HB).[41] PHA has been used to fabricate nerve conduits with good nerve regeneration capacity. NSCs seeded on PHA-based scaffolds showed good neurite connectivity, especially prominent on PHBHHx matrices. Also, cell viability and the propensity of NSCs' differentiation toward neuronal lineages are the highest on PHBHHx nanofibrous scaffolds, mainly due to the surface

topography and hydrophilicity of PHBHHx nanofibrous scaffolds. Scanning electron microscopy (SEM) showed that neurites could penetrate into the interior of PHBHHx nanofibrous scaffolds and establish close connections between cells, suggesting that the scaffolds provided positive cues for guiding the neurite outgrowth.

2.2. Nanopatterned Surfaces to Control Stem Cell Fate

Two main objectives of tissue engineering with stem cells are controlling proliferation without differentiation and inducing differentiation to specific lineages when desired. In addition to nanofibrous scaffolds, nanostructured surfaces have profound effects on stem cell behaviors.[15,42] Maintaining stem cell potency is important in order to expand the cells and obtain sufficient numbers for clinical therapies. Nanostructure surfaces can be used to either maintain stemness or induce differentiation (Figure 2b). Chen et al. investigated the influences of surface roughness (R), ranging from 1–150 nm, on ESCs' adhesion, spreading, and self-renewal.[43] They observed that undifferentiated cells preferentially adhered to smooth surfaces (R = 1 nm), and adhered less to surfaces with increasing roughness. In particular, smooth glass surfaces maintained the stemness and self-renewal capacity of ESCs in a long-term culture, whereas nanorough surfaces induced spontaneous differentiation.[43]

Using lithography methods, nanoscale patterns with precisely controlled dimensions and spatial orientation can be fabricated. Lee et al. reported that MSCs seeded on 350 nm ridge/groove pattern arrays (350 nm spacing, 500 nm height) elongated in the direction of the ridges/grooves, whereas cells seeded on flat surfaces had random orientation.[44] Additionally, the effect of nanopatterns was also evident on stem cell fate. For example, cells seeded on ridge/groove substrates differentiated into neuronal lineages in the absence of soluble inductive agents, while those on flat surfaces remained undifferentiated. These results were similar to stem cell behaviors on aligned nanofibers discussed previously.[34,35] In another study, Martino et al. investigated MSCs' behavior on hydrogenated amorphous carbon (a-C:H) films with grids, grooves, and flat surfaces. Interestingly, grooved nanopatterns guided the cell alignment in a similar manner as 350 nm ridge/groove patterns, but the grids did not.[45] Also, comparing 70/40 nm, 40/30 nm, and 30/20 nm (groove width/groove spacing) grooves demonstrated that cells elongated the most on 40/30 nm patterns. The results suggested that width and spacing dimensions are important parameters in directing stem cell fate. However, it is still unclear why grooves played a more active role in cell alignment than grids, what caused cells to elongate the most on 40/30 nm grooves, and why dimensions of grids (40/20 nm and 20/10 nm (square length/square spacing) had negligible effects on cell alignment and elongation.

In order to investigate the effects of different nanopatterns, You et al. fabricated nanostructured polyurethane (PU) substrates with dots (150, 400, and 600 nm diameter) and lines (150, 400, and 600 nm width).[42] In osteogenic media, MSCs on nanostructured substrates, except the 600 nm lines and dots, had a significantly higher ALP activity in comparison to the cells on unpatterned PU surfaces (controls). The highest differentiation propensity was observed on the 400 nm dotted surfaces, highlighting the ability of cells to sense the nanopatterns. It might be possible that the 400 nm dotted substrates mimic the surface roughness of natural bone. However, the reasons for the absence of ALP activity on 600 nm dot and line substrates are unclear. It could be related to cell attachment and penetration into nanostructured substrates, which need to be further investigated.

Besides width, spacing, and shape, height of nanopatterns also has significant influence on stem cell responses. Sjöström et al. fabricated titania nanopillars with 15, 55, and 100 nm heights on titanium (Ti) surfaces using anodization.[23] MSCs seeded on 15 nm patterns formed large focal adhesions with highly organized cytoskeletons. With an increase in nanopattern height, the focal adhesions shrunk and the cytoskeletons were less organized. Similarly, nanopatterns with 15 and 55 nm heights showed significantly enhanced cell spreading compared to nanopatterns with 100 nm pillars and polished Ti surfaces (controls). Thus, the increase in z-dimensions (up and down) of the nanostructures had impaired effects on cellular responses. However, it should be noted that lateral spaces between the ridges of the pillars were 12, 33, and 60 nm for the 15, 55, and 100 nm high nanopillars, respectively. Also, research has shown that spacing affects stem cell behaviors. Therefore, the observed results could be the combinative effects of height and spacing of nanostructures.[23]

Combinations of nano and micro features can provide important insight into stem cell response. Brammer et al. compared hydrophobic nanopillars (20 nm) with micropillars (2 μm); both had a height of 2.5 μm on silicon substrates.[46] Nanopillars were more hydrophobic than micropillars and showed enhanced MSC adhesion and growth compared to their micro-sized counterparts. The hydrophobicity and smaller features of nanopillars might affect density, conformation, and organization of adsorbed proteins, influencing cell adhesion. In particular, the dimension of 20 nm pillars is comparable to the typical size of globular proteins such that they might induce the high local protein density, thereby enhancing cell adhesion. In addition, cells on nanopillars formed large aggregates and their spreading was restrained. On the other hand, cells grew over and between micropillars as if they were not affected by the features. In the absence of biochemical-inducing reagents, MSCs seeded on nanopillar surfaces had dominant osteogenic differentiation among the three potential lineages of osteogenesis, chondrogenesis, and adipogenesis. Researchers hypothesized that cell aggregation on nanopillars is responsible for osteogenic differentiation since enhanced cell-cell interactions are expected to promote osteogenic differentiation. Nevertheless, restrained cell spreading is not typical for enhancing osteogenic differentiation, based on other studies, which showed that increased MSC spreading is linked to increased osteogenic differentiation.[46–48] This discrepancy might be attributed to the intrinsic non-uniformities of nanopillars created by an etching technique since nanoscale disorder alone could promote osteogenic differentiation.[48] It could also be due to the height of nanopillars; previous studies demonstrated that cell spreading decreased with the increasing height of nanopillars.[23,49] Although micropillars had the same height, the effects were likely compensated for by the effects of the microscale diameter.

In a similar study, Oh et al. created 30, 50, 70, and 100 nm TiO_2 nanotubes on Ti substrates.[50] The results showed that MSCs seeded on flat surfaces were round with minimum filopodia extensions while the cells seeded on nanotube surfaces were elongated. These morphology changes were more pronounced with increased tube diameter. Moreover, shortly after incubation, protein aggregates and deposits were found on TiO_2 nanotubes. With an increase in nanotube diameter, an increase in protein adsorption was observed, whereas significantly less protein was observed on flat surfaces.[50] These results contradicted the hypothesis suggested by Brammer et al. that protein aggregates would be more common on nanopillars/nanotubes with comparable sizes of protein aggregates (~20–30 nm in diameter), compared to larger structures.[46] However, it is possible that hydrophilicity of the surfaces might play an important role in protein adsorption. As a result of cell stretching/elongation, MSCs on large-diameter nanotubes underwent spontaneous osteogenic differentiation, whereas those on flat and 30 nm nanotube surfaces maintained their stemness.[50]

Spatial arrangement of nanofeatures could also be used to control stem cell fate and potency. McMurray et al. fabricated nanoscale PCL substrates with 120 nm pits in a square arrangement with 300 nm center-center spacing and investigated long-term maintenance of MSCs' multipotency.[51] The substrates with ±50 nm offset in a pit placement appeared to be osteogenic, whereas those with absolute square lattice symmetry permitted prolonged multipotency retention even when cultured in osteogenic media.

In conclusion, nanotopography could effectively control stem cell fate and self-renewal, even in the absence of differentiation-inducing reagents. However, there are some discrepancies between studies regarding cellular responses to particular nanotopography. Several factors could be responsible for these differences, including material characteristics, surface chemistry, mechanical properties, and uniformities of nanofeatures resulting from different fabrication techniques. The underlying mechanisms of the observed phenomena are still controversial, with many hypotheses needing further investigation.

3. Polymeric Nanomaterials for Stem-Cell-Based Tissue Engineering

Biological molecules such as growth factors (GFs) play critical roles in tissue engineering, and their presence in a controlled spatiotemporal manner is of key importance for directing stem cell fate.[19,52] GFs generally have a short half-life in circulation and undergo rapid degradation in vivo. Consequently, systemic/local infusion or bolus injection would be ineffective since stem cells often only respond to GFs above certain threshold concentrations. Repeated administration of GFs may cause toxicity due to accumulation of GFs or non-specific distribution. Moreover, GFs can poorly pass through cell membranes owing to their low diffusivity. Therefore, a delivery system is necessary to protect GFs from environmental factors and achieve a localized and controlled release.

Strategies for a sustained GF delivery include direct entrapment or chemical conjugation to scaffolds, and micro/nanoparticulate systems, which can be added to the culture medium or incorporated into scaffolds and hydrogels.[19,52] Direct entrapment or covalent conjugation of GFs to scaffolds has been shown to provide sustained releases. However, the control over release kinetics is limited. Therefore, micro/nanoparticles as GF carriers, of which release kinetics can be easily tuned while minimally interfering with scaffold properties, have gained increasing interest. Compared to microparticles, nanoparticles (NPs) have enhanced transport properties and pharmacokinetic profiles due to a high surface-to-volume ratio. In particular, nanoparticles have a higher loading capacity and can more easily pass through lipid membranes, as well as penetrate deeper into tissues. Nanoparticulate systems for GF delivery developed to date include polymer-based, lipid-based, and other miscellaneous systems. Among these, polymeric nanoparticles in the forms of nanospheres, nanocapsules, micelles, and dendritic particles have been extensively studied.

3.1. Polymeric Nanoparticles as Bioactive Factor Carriers

Polymeric nanoparticles can provide sustained GF release to effectively control stem cell fate. For example, hepatocyte growth factor (HGF) was loaded into chitosan nanoparticles (CNPs) by an ionotrophic gelation method, with particle sizes of ≈20–50 nm.[53] The monophasic-sustained release of HGF was observed with 85% of HGF released after 5 weeks. HGF-CNPs were added to the culture medium, and after 21 weeks in culture, MSC morphology changed from fibroblast-like to a round shape, characteristic of hepatic cells. Hepatic differentiation was confirmed by increased expression of albumin. Interestingly, cells in the medium supplemented with an epidermal growth factor (EFG) (positive controls) were differentiated to a greater extent than those with HGF-CNPs, perhaps due to the higher concentration of GFs in the positive controls compared to the amount released from nanoparticles. The retention of GF might be attributed to the strong electrostatic interactions between positive-charged chitosan and proteins.[53] Pulavendran et al. conducted further studies by injecting MSCs together with HGF-CNPs into mice with liver cirrhosis.[54] HGF-CNPs effectively enhanced hepatic differentiation of MSCs and induced the reversal of fibrolysis of liver ECM in vivo.[54] However, HGF-CNPs were not compared with the direct injection of HGF, and thus the superior performance of CNPs' delivery system in vivo could not be clearly inferred.

Similarly, Santos et al. used retinoic acid (RA)-loaded, polyethylenimine (PEI)/dextran sulfate (DS) nanoparticles to induce differentiation of neural stem cells in the subventrical zone (SVZ) of the brain.[55] SVZ cells readily internalized RA-NPs and the released RA interacted with the RA receptor (RAR) and subsequently activated the stress-activated protein kinases (SAPK)/Jun amino-terminal kinases (JNK) signaling pathway. This turned on preneurogenic genes that promoted axonogenesis and axon outgrowth. Moreover, RA-NPs could induce proneurogenic effects using an RA concentration approximately 2500-fold lower than the solubilized RA. The results indicated that the epigenetics behind neuronal differentiation by RA-NPs and solubilized RA are different. In particular, NSCs are a heterogeneous cell population that may differentially respond to RA-NPs and free RA. It was postulated that RA-NPs might be

able to target a broader population of SVZ cells than free RA. It is promising that the system may offer a new perspective for treatments of neurodegenerative diseases.[55]

In a similar approach, dexamethasone-loaded carboxymethylchitosan/poly(amidoamine) dendrimer NPs (Dex-loaded CMCht/PAMAM) were employed for osteogenic differentiation of rat bone marrow stromal cells (RBMSCs).[56] Oliveira et al. reported that NPs were internalized with high efficiency and did not cause any adverse effects up to the concentration of 1 mg/mL. In addition, mineralization, ALP activity, and osteocalcin expression of RBMSCs seeded on scaffolds loaded to Dex-loaded CMCht/PAMAM NPs were comparable to cells cultured in standard osteogenic media. In vitro release studies revealed that the concentration of Dex released from NPs is similar to osteogenic media. The NPs could be used for spatially controlled differentiation if contained within a scaffold or hydrogel. Additionally, osteogenic media would need to be replenished after every 2–3 days, whereas a single dose of NPs is sufficient to induce osteogenic differentiation of stem cells.[56]

In addition to conventional NPs, core-shell NPs could provide an additional level of controlled release. Haidar et al. fabricated a core-shell nanoparticulate system consisting of a positively charged unilamella liposome core and a shell of alternating layers of positively charged chitosan and negatively charged sodium alginate.[57] The resulting NPs showed a shelf-life of up to 12 months, which allowed immediate GF loading before future administrations. The core-shell design offered copious compartments for BMP-7 entrapment, resulting in a sustained GF release over 45 days (i.e., an initial burst followed by a slow release). Liposomes with three and five alginate-chitosan layers with a maximum loading capacity of ≈40% were used for the studies. The loading capacity could be enhanced up to 80% with a 10-layer shell, but the particle size grew beyond nanoscale. Also, the results showed that particles with five layers exhibited a slower release profile compared to particles with three layers, illustrating the capability to fine-tune the release of therapeutics. Preosteoblasts cultured with BMP-7 loaded NPs showed significantly higher ALP activity than ones supplemented with solubilized BMP-7, suggesting effective osteogenic differentiation by the NP system.[57]

Besides GFs, transcription factors (TFs) can be effectively delivered using NPs to direct the differentiation of stem cells/progenitor cells. For example, polyethylene glycol-based protein nanocapsules with sizes of ≈10–20 nm are used for delivery of recombinant myogenic transcription factors (myoD) to induce myogenic differentiation of progenitor cells.[58] Nuclear localization of myoD is enhanced due to the nanocapsules delivery in comparison to native myoD, mainly due to the fact that although native myoD can penetrate the cell membrane, the protein gets entrapped in endosomes and degrades during the internalization. The use of nanoparticles provides a physical barrier and preserves the activity of myoD. Nanocapsules loaded with myoD effectively induce myogenic differentiation compared to native myoD, as evidenced by the elongated and multinuclear morphologies, which are the hallmarks of myotubes (skeletal lineage). The use of native myoD displays low levels of myosin heavy chain (My-HC) in progenitor cells, and elongated multinucleated myotubes morphology is also absent. The incomplete differentiation by native myoD may correlate to a limited activity of myoD delivered to nuclei.[58]

Nanoparticles are internalized via different endocytosis pathways, and cellular internalization of nanoparticles is significantly influenced by hydrophobicity, softness, shape, and surface chemistry of nanoparticle surfaces.[59–62] Effects of these factors on cellular uptake are illustrated in **Figure 3**.The size of NPs has been shown to have minor influences on cellular uptake, as long as they are in the range of 50–200 nm. Lorenz et al. reported that NPs made from softer and more hydrophobic polymers were taken up to a greater extent.[59] For example, hydrophobic nanoparticles synthesized from poly(n-butyl methacrylate) (PBMA), poly(hexyl methacrylate) (PHMA), and poly(lauryl methacrylate) (PLMA) are internalized more easily compared to hydrophilic nanoparticles fabricated from poly(methyl methacrylate) (PMMA), poly(propyl methacrylate) (PPMA), and poly(stearyl methacrylate) (PSMA). Hydrophobicity controls nanoparticles' interactions with components of the cellular microenvironment, including serum proteins and lipid membranes, and ultimately, intracellular uptake. The rationale behind the enhanced cellular uptake by softer nanoparticles is unclear, but it is hypothesized that soft nanoparticles could deform easily upon cellular contact, leading to a more favorable interaction with cell membranes in comparison to their harder counterparts (Figure 3a). Interestingly, poly(t-butyl methacrylate) (PtBMA) NPs were internalized extremely well by MSCs, compared to other poly(alkyl methacrylate) NPs and other cell lines, perhaps due to the hydrolysis of tert-butyl ester groups, which resulted in carboxylic acids and carboxylated nanoparticles being internalized by MSCs readily compared to plain polymeric NPs (Figure 3b). Since PtBMA NPs are not taken up as well by other cell types, they have the potential to be used for MSC targeting.[59]

In another study, the effect of shape of nanoparticles was shown to have significant influences on cellular uptake. Florez et al. revealed that spherical NPs were readily taken up by MSCs and HeLa compared to their quasi-ellipsoid counterparts.[60] The uptake of NPs decreased with an increase in the aspect ratio (polar axis:equatorial axis). These phenomena could be explained by the fact that cells needed to wrap around the polar axis (pole) of NPs during internalization. The stretched nanoparticles preferentially absorbed on the cell membrane along their polar axis, thereby making it more difficult for the highly stretched nanoparticles to be taken up.[60] Furthermore, Jiang et al. compared intracellular uptake of polystyrene nanoparticles and amino-functionalized polystyrene nanoparticles by MSCs to investigate the effects of surface amines on cellular internalization.[61] Since proteins were known to be adsorbed on nanoparticle surfaces to form a so-called "protein corona," they were expected to likely influence cells/nanoparticles' interactions. The results showed that amino-functionalized polystyrene nanoparticles were taken up rapidly compared to polystyrene nanoparticles. The amino-functionalized polystyrene nanoparticles were taken up via a cadherin-mediated endocytosis, whereas polystyrene nanoparticles were taken up via a cadherin-independent pathway, mainly due to specific interactions between amine groups on nanoparticle surfaces and cell endocytosis machinery.[61,62]

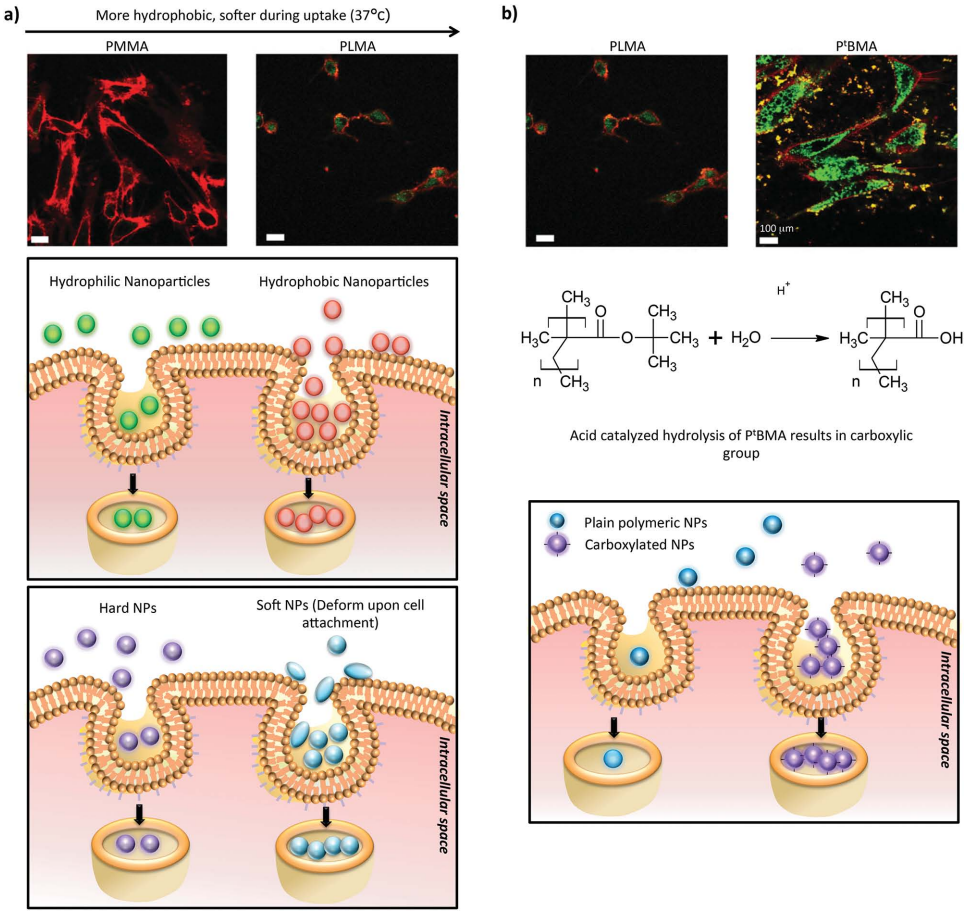

Figure 3. Effects of hydrophobicity, softness, and surface chemistry of nanoparticles on cellular internalization. For example, a) PLMA was more hydrophobic and softer than PMMA at 37 °C, thus, was more internalized. The nanoparticles were shown in green and cell membrane in red. Hydrophobicity influences how nanoparticles interact with their environments, including serum proteins and lipid membranes. More hydrophobic nanoparticles are taken up to a greater extent (upper panel). Soft nanoparticles can deform upon cell attachment, leading to a more favorable interaction with cell membranes. Consequently, they are taken up more than their stiffer counterparts (lower panel). Surface chemistry was also shown to influence cellular uptake. For example, b) P^{t}BMA nanoparticles were taken up significantly more than PLMA. This was attributed to the hydrolysis of P^{t}BMA in a mild acidic media, resulting in a carboxylic group. Carboxylated nanoparticles were reported to be internalized to a greater extent than the plain ones. Reproduced with permission.[59] Copyright 2010, John Wiley & Sons, Inc.

In a similar study, Zhang et al. evaluated cellular uptake of polystyrene nanospheres (20 nm diameter) and nanodiscs (20 nm diameter and 2 nm thickness).[63] Nanospheres were readily internalized into HeLa cells, whereas nanodiscs were primarily associated with cell membranes (**Figure 4**a). Studies with artificial membranes showed that the capability of nanospheres to cross lipid bilayers was six times higher than that of nanodisks, while membrane retention of nanodiscs was eight times higher. It was hypothesized that the strong association of nanodiscs with membranes disturbed the lipid's arrangement, i.e., reduced the orderliness of lipids, thereby allowing the nanodiscs to get inside the bilayers. In addition, because nanodiscs were thinner (2 nm) than cell membranes (5 nm) and anisotropic in shape, they might have stayed inside the bilayers and seldom entered cells. As a consequence of lower internalization, nanodiscs did not induce reactive oxygen species (ROS) generation and apoptosis.[63] Nevertheless, these scenarios could be different if nanodiscs were thicker than lipid bilayers.

In addition, Agarwal et al. reported that endothelial, epithelial, and immune cells preferentially internalized polyethylene glycol diacrylate (PEGDA)-based nanodiscs over cuboidal (quadrilateral cross-section) nanorods for disc-rod pairs with equivalent volumes.[64] The nanodiscs were 70–100 nm thick, significantly thicker than those used by Zhang et al.[63] (2 nm). As a consequence of the increased thickness, they were internalized instead of residing in lipid bilayers (Figure 4b,c).[63,64] Large nanodiscs and nanorods were more effectively taken up by cells compared to their smaller counterparts, and small nanospheres were internalized more than larger ones. These effects resulted from complex interplay between the surface area in contact with the cell membranes and strain energy required for membrane deformation. Specifically, larger discs and rods had larger surface-contact areas, which may have resulted in stronger adhesion force and subsequently promoted initial cellular uptake. This effect was minimal for nanospheres, where the increase in size had little effect on surface-contact areas. Smaller spheres were readily internalized since the

strain energy required for bending the membranes was lower. For discs and rods with equivalent volume and surface area in contact with cells, discs were taken up more readily due to the lower energy.[64]

In Agarwal et al.'s study, longer nanorods were internalized more than their shorter counterparts.[64] The results might seem counterintuitive to those reported by Florez et al., where the uptake of quasi-ellipsoids decreased with an increase in aspect ratio (polar axis:equatorial axis).[60] However, the nanorods in this study had quadrilateral cross-sections that might have created different effects on cellular uptake compared to quasi-ellipsoids in the study by Florez et al., which could be thought of as stretched nanospheres.[60] It is possible that for quasi-ellipsoids, the effects of increased energy cost dominated the effects of increased surface area, similar to the case of nanospheres. The studies by Zhang et al. and Agarwal et al. were not tested on stem cells, and some of these phenomena might be cell specific.[5,63,64] Nevertheless, they provide certain guidelines for nanomaterial designs with respect to cellular internalization.

3.2. Polymeric Nanoparticle-Loaded Scaffolds

One of the challenges while using NPs for in vivo delivery includes lack of control over localized delivery. Use of polymeric matrices can be used to deliver NPs locally for tissue engineering applications. In a recent study, platelet-derived growth factor (PDGF)-loaded poly(lactic-co-glycolic acid)-monomethoxy-poly(ethylene glycol) (PLGA-m-PEG) NPs (≈150 nm) were incorporated within nanofibrous collagen scaffolds.[65] The controlled release of PDGF was used to induce tendogenic differentiation of adipose-derived stem cells (ASCs).[65] NPs were formed by double emulsion techniques, and NP-collagen fibers were created by electrochemical process. NP-loaded scaffolds showed an initial burst release of PDGF followed by a sustained released for up to 42 days. Controlled release of PDGF from NPs resulted in tendogenic differentiation, as observed by the enhanced expression of tendon markers on cells seeded on fibrous scaffold. The fibrous collagen scaffold reported here was not covalently crosslinked, and the crosslinking of collagen would not only improve mechanical integrity of the scaffolds but can also provide control over the release of entrapped PDGF.

In order to stimulate strong cellular responses, sequential deliveries of GFs are required. For example, in osteogensis, simultaneous delivery of BMP-2 and BMP-7 have significantly stronger influence on cell proliferation and differentiation compared to single GF delivery.[66] In a recent study, Yilgor et al. fabricated BMP-2-loaded PLGA nanocapsules and BMP-7-loaded PHBV nanocapsules and entrapped the nanoparticles within chitosan-based scaffolds.[66] PLGA- and PHBV-based nanocomposites have different degradation profiles and thus can be used to deliver GFs in a sequential pattern. Three delivery modes were compared: single BMP-2/BMP-7, simultaneous BMP-2 and BMP-7 (both GFs in PLGA nanocapsules), and sequential BMP-2 followed by BMP-7 delivery. The results indicated that MSCs seeded on BMP-2-loaded nanocapsules had lower proliferation and higher ALP activity than the ones on BMP-7-loaded nanocapsules, whereas simultaneous delivery yielded a higher ALP activity than BMP-7 nanocapsules but lower than BMP-2-nanocapsules. Most importantly, sequential delivery resulted in a significantly higher degree of osteogenic differentiation, suggesting the importance of GF delivery in a spatiotemporally controlled manner.[66]

In a similar study, Dyondi et al. fabricated injectable gellan, xantan-based hydrogels loaded with chitosan NPs.[67] Chitosan NPs act as a dual GF delivery system for promoting differentiation of fetal osteoblasts. BMP-7/bFGF-loaded chitosan NPs showed a sustained release profile compared to free GFs in hydrogels. The sustained release of GFs resulted in significantly higher calcium deposition on hydrogels loaded with GFs. Earlier studies have shown that chitosan upregulates several osteogenic genes associated with matrix mineralization. Thus, the increase in calcium deposition on nanocomposite hydrogels could be attributed to the combinatorial effects of GFs and a chitosan matrix.[67]

Overall, GF-loaded nanoparticles can be incorporated within different scaffold structures such as fibrous scaffolds, hydrogels, and porous scaffolds to direct stem cell differentiation. By controlling the release of GFs from NPs, different cellular processes can be enhanced or suppressed. A range of strategies can be employed to control the delivery of growth factors in a sequential manner to mimic or enhance native microenvironments.

3.3. Polymeric Nanofibers as Delivery Systems

Besides using NPs as GF carriers, direct entrapment and chemical conjugation of GFs to scaffolds have been shown to provide sustained releases. Jiang et al. encapsulated RA within PCL/gelatin nanofibrous scaffolds. A sustained release was obtained for at least 14 days with a cumulative release of 60%. By combining nanotopography with sustained RA release, neuronal marker expressions were enhanced compared with bolus delivery.[68] Similarly, Horne et al. demonstrated that tethering brain-derived neurotrophic factors (BDNF) to PCL nanofibrous scaffolds enhanced NSCs' proliferation and differentiation toward neurons and oligodendrocytes, compared to culturing with soluble BDNF in the media.[69] Nerve growth factor (NGF) was also conjugated to electrospun, amine-functionalized, PCL-PEG block co-polymers. Cho et al. showed that conjugated BDNF had superior bioactivity compared to the factors directly adsorbed onto the fibers, resulting in a higher expression of neuronal markers.[70]

To overcome low drug-loading capacity, burst release, and limited control of release kinetics associated with electrospun nanofibers as delivery carriers, core-shell nanofibers have been introduced. Not only do they protect GFs from a harsh environment and provide a sustained release, but they also allow modifications of delivery systems while minimally affecting core materials.[71,72] For example, Su et al. studied the controlled release of Dex and BMP-2 from core-shell PLLACL-collagen nanofibers. It was found that Dex and BMP-2 released from core-shell nanofibers were sustained longer than those released from PLLACL/collagen blend electrospun fibers. Furthermore, three modes of delivery were investigated: Dex and BMP-2 in the core, Dex in the shell and BMP-2 in the core, and Dex and

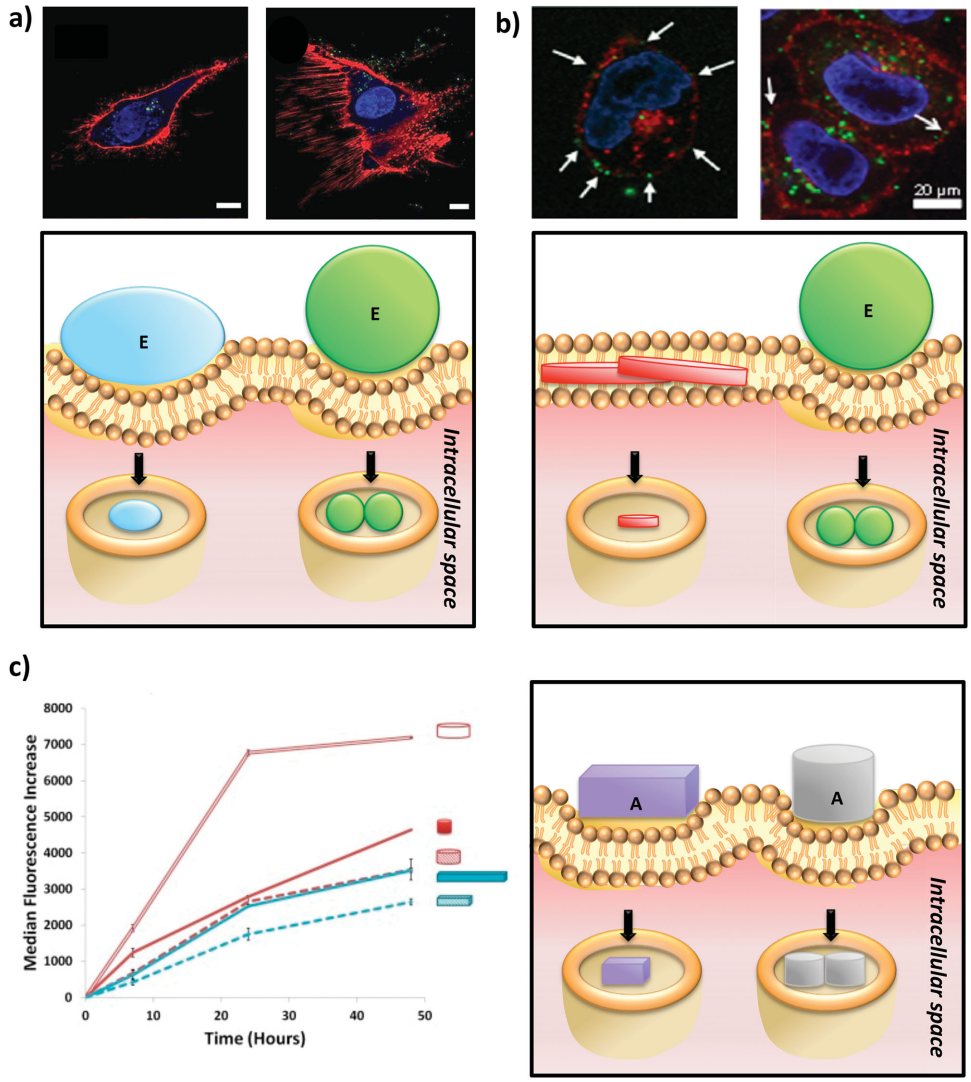

Figure 4. Effects of shape of nanoparticles on cellular uptake. Note that nanoparticles are were shown in green, cell membrane in red; and white arrows pointed to nanoparticles attached to the membrane. The comparative extent of internalization was resulted from complex interplay between strain energy required for membrane deformation and surface area of contact. The dominant factor for each shape is designated with either E or A. a) Spherical nanoparticles were internalized more than quasi-ellipsoids; and the uptake of quasi-ellipsoids decreased with increasing aspect ratio (polar axis:equatorial axis) due to the higher energy required to wrap cell membranes around the particles. b) Nanodiscs which are thinner than cell membranes tended to stay inside the bilayers and seldom entered cells. c) On the other hand, nanodiscs significantly thicker than cell membrane were readily internalized, and to a greater extent than cuboidal nanorods with an equal volume. Reproduced with permission.[61,63] Copyright 2010 and 2012, American Chemical Society.

BMP-2 in the shell. It was apparent that for the BMP-2-core/Dex-shell case, Dex displayed a more initial burst release followed by a slower increase. When Dex and BMP-2 were in the same compartment, the BMP-2 release was slightly faster with a higher final accumulative release than Dex. The release kinetics were mainly influenced by diffusion and polymer degradation. In particular, drugs initially diffused through pores of fibers and then changed to a combined diffusion/erosion mechanism. Moreover, cell studies showed that ALP activity, and hence, the extent of osteogenic differentiation, was proportional to the amount of drugs released at a particular time point. Interestingly, MSCs cultured with solubilized Dex and BMP-2 (tissue culture polystyrene (TCP) controls) were more differentiated than those on core-shell nanofibers. One possibility was that changing the medium in the first 7 days of culture removed an initial burst of BMP-2 and Dex, and thus their concentration in the medium was lower than that available in TCP controls.[71]

In addition to core-shell design, depot-like amphiphilic scaffolds have been shown to prolong the release of bioactive factors (**Figure 5**).[73] Recently, sustained release of Dex from beaded electrospun poly(ethylene oxide terephthalate)-poly(butylene terephthalate) (PEOT/PBT) scaffolds was reported.[73] Amphiphilic beads served as drug reservoirs integrated within nanofibers. An initial burst followed by sustained release of Dex for up to 4 weeks was observed. MSCs seeded on the scaffolds showed enhanced ALP activity and formation of a

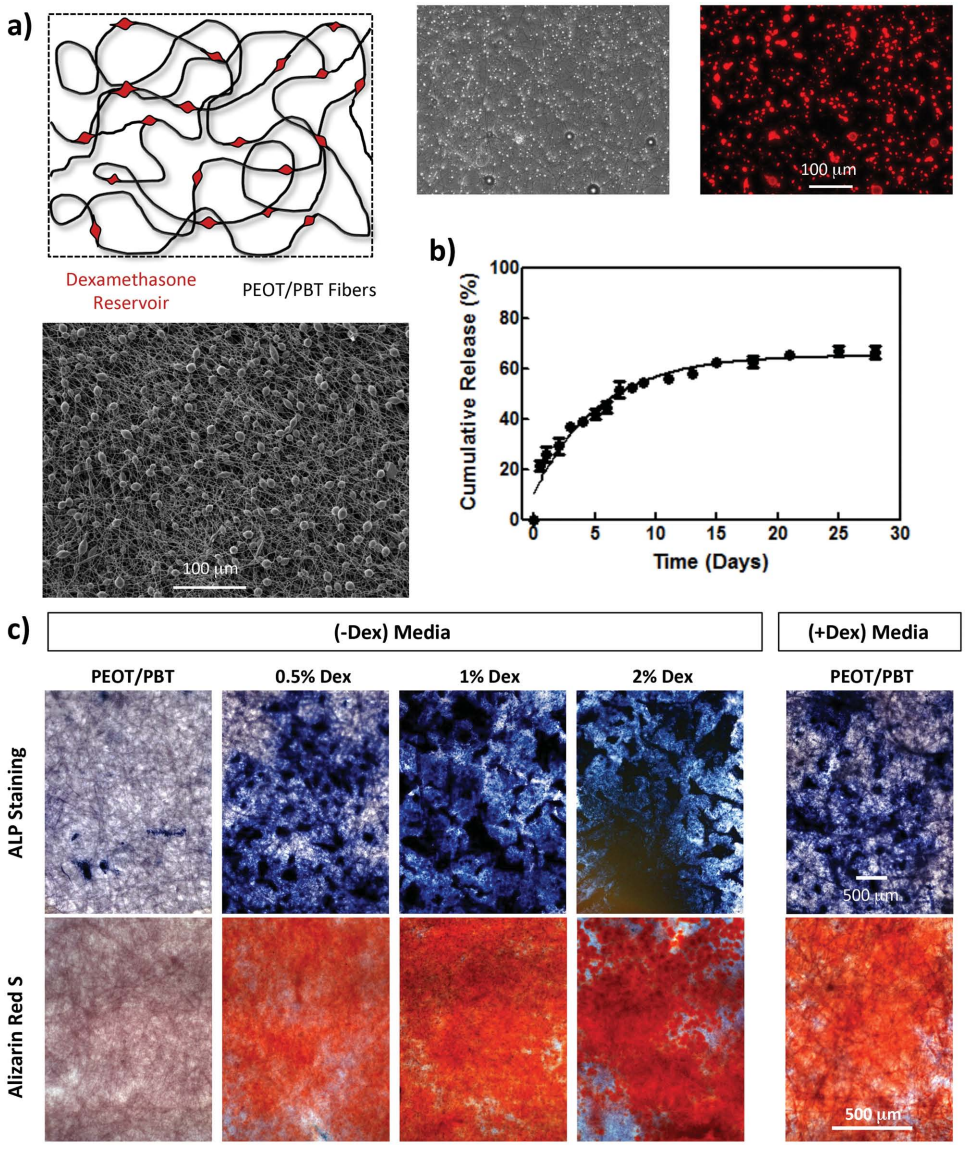

Figure 5. Nanofibrous scaffolds for control release of drug to induce osteogenic differentiation of stem cells. a) Beaded structure integrated within fibrillar scaffolds act as a drug depot for control release of dexamethasone. Imaging techniques reveal distribution and localization of drug (red) within the beaded structures. b) Control release of dexamethasone was over a period of three weeks. c) The controlled release of dexamethasone induces osteogenic differentiation of human stem cells as evident by increase in ALP straining and formation of mineralized matrix (red stain) after 28 days. Reproduced with permission.[73] Copyright 2014, Elsevier.

mineralized matrix, indicating osteogenic differentiation when compared to bolus delivery of Dex in culture media.[73] This study highlighted that, as expected, sustained release of drug can perform better compared to bolus delivery for controlling stem cell differentiation.

Overall, polymeric nanomaterials have been demonstrated to possess enormous potential to overcome limitations of conventional delivery systems. So far, the choice of materials has been relatively limited, especially for making NPs. Nevertheless, engineering different sections of delivery systems, for example, dual/sequential delivery, and targeting ligands for combinatorial effects would offer great flexibility in designing polymeric NPs for particular applications in the future.

4. Ceramic-Based Nanomaterials

4.1. Nano-Hydroxyapatite

Bioactive nanoceramics such as hydroxyapatite, bioactive glasses (BG), nanosilicates, and silica nanoparticles (SiNPs) have been widely used for hard tissue engineering owing to their bioactive characteristics. Among these materials, nano-hydroxyapatite (nHA) has been extensively studied due to its similar chemical composition and structure to bone minerals. Due to its similarity with native tissue components, it is expected that stem cells might be able to recognize the chemical structure of the nanomaterials and might facilitate osteogenic differentiation.

In a recent study, Lee et al. reported that MSCs seeded on PLGA/nHA nanofibrous scaffolds showed upregulation of ALP activity, production of mineralized tissue, and osteogenic gene expressions, compared to cells seeded on PLGA scaffolds,[74] a finding mainly attributed to the osteoconductive property of nHA and increased protein adsorption on PLGA/nHA nanofibers. Typically, proteins tend to favorably adsorb on hydrophilic surfaces, and previous studies have shown that the addition of nHA increased the hydrophilicity of macroporous scaffolds, enhancing serum protein adsorption. In this study, nHA had negligible effects on hydrophilicity of nanofibers. Therefore, it was postulated that the increased protein adsorption was rather a consequence of nanofiber roughness in the presence of nHA. Parameters, which affect protein adsorption, could be further investigated. In a similar approach, Xue et al. proposed using porous PLGA/nHA hybrid scaffolds for osteochondral regeneration.[75] They reported that cell attachment, viability, and proliferation on PLGA/nHA scaffolds were significantly higher than those on PLGA counterparts. In vivo studies showed that cartilage defects in rats treated with PLGA/nHA were completely repaired with regenerated hyaline cartilages after 12 weeks. On the other hand, for PLGA groups, the newly formed tissues were mainly fibrocartilages without obvious bone formation. Despite promising results, designing gradients in structure and composition of engineered tissue is a challenge, and other fabrication technologies need to be looked at to mimic tissue interfaces.

In addition, PCL/Col/nHA nanofibrous scaffolds were shown to better support MSC spreading and proliferation than PCL, Col, and PCL/nHA scaffolds. Also, vitronectin (VN) and fibronectin (FN) adhesions were markedly greater on the tri-component scaffolds. These results agree with the fact that VN and FN promote integrin-dependent cell adhesion and proliferation, as well as osteogenic differentiation. Interestingly, cells failed to adhere and survive on Col scaffolds despite the presence of integrin receptors, possibly due to low tensile modulus of non-crosslinked collagen since it has been established that substrates that are too elastic can induce cell apoptosis; however, this hypothesis needs to be further investigated.[76] Furthermore, Yang et al. studied behaviors of dental pulp stem cells (DPSCs) on PCL/gelatin/nHA scaffolds. It was reported that cells seeded on PCL/gelatin/nHA scaffolds showed a greater extent of odontoblastic differentiation than cells on PCL/gelatin scaffolds in vitro. In addition, DPSC-seeded scaffolds were implanted into mice. A hard tissue formation was observed on all scaffolds, with no significant differences between those with and without nHA. Moreover, there was a negligible tissue ingrowth for all scaffolds, which might have contributed to the limited effects of nHA in vivo. Although the addition of nHA enhanced cell differentiation in vivo, it had no advantage for cell adhesion and growth, which is discrepant with other studies that showed that the addition of nHA enhanced cell adhesion and growth. The authors explained that when nHA was added to hydrophobic nanofibers, the hydrophilicity was increased, affecting cellular responses. In contrast, since PCL/gelatin was already hydrophilic, the increased hydrophilicity from the nHA addition had negligible effects.[77] However, effects of nHA on hydrophobicity of nanofibers are controversial; the study by Phipps et al. showed that the addition of nHA to hydrophilic nanofibers increased cell spreading and proliferation.[76] Thus, the underlying reasons for these observations are still unclear.

Besides incorporation of nHA to scaffolds, nHA coatings enhance osteogenic differentiation of stem cells. For example, Zandi et al. evaluated cytocompatibility of nanorod HA/gelatin scaffolds coated with nHA by chemical bath deposition.[78] In comparison with spherical and mixed-shape nHA, nanorod HA was better distributed in gelatin due to its higher specific surface area, resulting in higher reactivity. Scaffolds with and without nHA coatings provided an appropriate environment for MSC proliferation, with more cells on the coated surfaces, mainly due to enhanced surface area in the presence of nano-sized HA.[78] Similarly, nHA was precipitated on poly(L-lactic acid)/Poly-benzyl-L-glutamate/Collagen (PLLA/PBLG/Col) scaffolds by a calcium phosphate dipping method.[79] The proliferation rate of ASCs was higher on PLLA/PBLG/Col/nHA than on PLLA/PBLG/Col. Additionally, ALP activity, calcium deposition, and osteogenic gene expressions were higher on PLLA/PBLG/Col/nHA scaffolds.[79]

Electrospinning of polymer/nHA solutions and coating scaffolds by nHA precipitation have been shown to enhance osteogenic differentiation. However, these methods have some drawbacks. Specifically, embedding nHA inside fibers might mask its bioactivity. In the latter method, time to achieve a stable apatite deposition is increased and aggregated CaP might interfere with porous structures of scaffolds, hindering cell infiltration. Therefore, Seyedjafari et al. coated PLLA nanofibers by direct deposition of nHA and investigated behaviors of seeded somatic stem cells.[80] Using direct deposition, it was expected that weakly bound nHA would be detached from scaffolds after rinsing several times, thereby not blocking the pores. The results showed that nHA had no effects on cell proliferation, and the proliferation rate on PLLA/nHA and PLLA was lower than that on TCP. The osteogenic differentiation of stem cells was the most pronounced on PLLA/nHA, followed by nHA and TCP, respectively. Interestingly, there was no difference on the messenger RNA (mRNA) levels of runt-related transcription factor 2 (Runx2), a transcription factor that involves an orientation of stem cells toward osteogenic lineage, between PLLA/nHA and PLLA. This finding suggests that nHA induced osteogenic differentiation by upregulating mRNA of ALP and osteocalcin, for instance, rather than Runx2,[80] and agrees with work by Lin et al. on the inability of nHA to upregulate the Runx2 expression of stem cells.[81]

In some studies, use of growth factors along with nHA has shown promising results. Liu et al. reconstructed alveolar bone defects using a DPSC-seeded Col/PLLA/nHA hybrid loaded with BMP-2.[82] The hybrid scaffold induced faster mineralization, compared with nHA/Col/PLLA, nHA/Col/PLLA/BMP-2, nHA/Col/PLLA/DPSCs, and autologous bone. Although the defects were not completely closed after 12 weeks of surgery, the hybrid might offer an alternative to autologous bone.[82]

4.2. Bioactive Glasses

Bioactive glasses, degradable glasses in a Na_2O–CaO–SiO_2–P_2O_5 system, are reported to stimulate bone formation and rapidly bond with surrounding bone. Despite their relatively complex

chemistry and difficulty in processing, bioactive glasses have received significant interest in the past decade.[83] However, very few reports focus on understanding and evaluating the interactions between nano bioactive glasses (nBGs) and stem cells. Jones et al. investigated the interactions of nBGs (~250 nm) with MSCs and monitored the cellular trafficking.[84] nBGs are internalized by endocytosis and accumulate inside endosomes in cytoplasm. In some instances, randomly distributed nBGs were observed between actin filaments, suggesting that they might have escaped from endosome. The increase in nBG concentration resulted in a decrease in metabolic activity and proliferation in a dose-dependent manner; however, nBG was not cytotoxic up to the tested concentration of 200 μg/mL. Internalized nBG appeared to dissolve inside MSCs, leading to increased concentrations of soluble calcium and silica. Since intracellular calcium concentration plays a critical role in regulating oxidative stress and cell death, this might explain the reduced metabolic activity of MSCs upon nBG exposure.[84] In another study, Hong et al. studied the effects of nBGs on stem cells' biomechanics.[85] The addition of nBGs resulted in a significant decrease in plasma membrane stiffness of MSCs by ≈50%, suggesting that calcium and silicon (ionic dissolution products of nBGs) might alter biomechanical properties of MSCs, thereby facilitating membrane protrusion and cell spreading. Although this study shed some light on the interactions between nBGs and stem cells, it is essential to determine the role of enhanced intracellular mineral concentration in controlling cell fate.

A range of bioactive nanocomposites have been fabricated by combining nBGs with synthetic and natural polymers. In a recent study, Mota et al. designed chitosan/nBG nanocomposite membranes and investigated their interactions with MSCs and periodontal ligament cells (PDLs).[85] The results showed that the addition of nBGs enhances PDLs' proliferation but not MSCs'. The exact mechanism of cell adhesion on chitosan/nBG nanocomposite surfaces is unclear, and additional studies need to be performed. Nevertheless, both MSCs and PDLs seeded on chitosan/nBG had higher calcium concentration than MSCs seeded on chitosan membranes, suggesting enhanced mineralized matrix production.[85] In a similar study, Hong et al. reported synthesis and fabrication of collagen (Col)/nBG nanofiber scaffolds for MSC adhesion, proliferation, and migration.[86] The addition of nBG to the Col resulted in a significant increase in ALP activity compared to pure Col scaffolds, which might be attributed to the ionic dissolution products of bioactive glasses that upregulate gene expression and promote osteogenic differentiation of stem cells. It is also believed that the ionic dissolution products precipitate from the solution and create an appropriate surface topography and microenvironment for enhanced cell attachment and matrix formation.[86] Despite the potential of nBG for tissue engineering applications, the localized increase in ionic concentration and long-term fate of nBG under in vivo conditions need to be investigated in detail.

4.3. Synthetic Silicates Nanoparticles

Synthetic silicate nanoparticles (nanosilicates) are two-dimensional nanomaterials with 20–30 nm diameters and 1 nm thickness. Due to the unique shape and surface charge of these silicate nanoparticles, they interact with stem cells in a substantially different manner compared to other types of nanoparticles. The interaction of nanosilicates with MSCs and ASCs over a period of 28 days was investigated (**Figure 6**).[20,87,88] At a lower concentration (100 μg/mL), no significant effect was observed in cellular morphology, proliferation, viability, and production of ROS and reactive nitrogen species (RNS).[20] However, at higher concentrations, a significant reduction in metabolic activity was observed. Half-maximum inhibitory concentration (IC_{50}), the concentration of nanosilicates at which metabolic activity of MSCs was reduced to 50%, was found to be 4 mg/mL.[20] Compared to nHA and SiNPs with similar size, nanosilicates, showed cytotoxicity at a ten-fold higher concentration, indicating relatively high cytocompatibility.[20] These nanosilicates are primiraly internalized by cell vial clathrin mediated endocytosis (Figure 6b).[87] Researchers also showed that the addition of nanosilicates to MSCs upregulated ALP production, osteocalcin, osteopontin, and Runx2 in the absence of any osteoinductive growth factors such as Dex and BMP-2 (Figure 6c).[20,87] The osteoinductive characteristic of nanosilicates is attributed to their dissolution products—Na^+, Mg^{2+}, $Si(OH)^4$, and Li^+—which might promote osteogenic pathways. In particular, orthosilicic acid ($Si(OH)_4$) upregulates bone-related gene expressions and promotes collagen I synthesis,[89] and Li^+ activates Wnt-responsive genes by regulating the Runx-2 transcription factor.[90]

In another study, the interaction between nanosilicate-loaded nanocomposites and stem cells was investigated.[91] They fabricated physically crosslinked silicate-poly(ethylene oxide) (PEO) nanocomposite films and showed that at high silicate concentrations (60% and 70%), MSCs prefer to attach to a nanocomposite surface. In nanocomposites with low silicate concentrations (40% and 50%), where non-cell-adhesive PEO chains dominated, cells growth was limited. Because PEO is non-cell adhesive, the addition of silicates can be used to control cell spreading and proliferation. A significant increase in MSCs' attachment, proliferation, and osteogenic differentiation was also observed due to the addition of nanosilicates, which was mainly attributed to enhanced protein adsorption on nanosilicates present on nanocomposite surfaces.

In addition, Wang et al. incorporated nanosilicates into electrospun PLGA nanofibers.[92] Researchers found that more serum proteins were adsorbed on PLGA/nanosilicates than on pure PLGA nanofibers, possibly as a consequence of a slight increase in hydrophilicity and an expansion of nanofibers upon LAP addition, making them more favorable for protein adsorption. As a result, cell adhesion and proliferation were enhanced.[92] Similarly, Gaharwar et al. reported that the addition of nanosilicates to electrospun PCL induced osteogenic differentiation.[93] The nanosilicates supported adhesion and proliferation of hMSCs. Also, osteogenic differentiation increased with nanosilicates contents increasing from 0.1% to 10%, as evidenced by enhanced ALP activity and matrix mineralization. Since protein adsorption was comparable among samples, it was postulated that enhanced differentiation was mainly attributed to increased surface roughness with increasing nanosilicate content. It was shown that cells preferably anchor and stretch their filopodia on a microscale rough surface, leading to enhanced metabolic activity.[93]

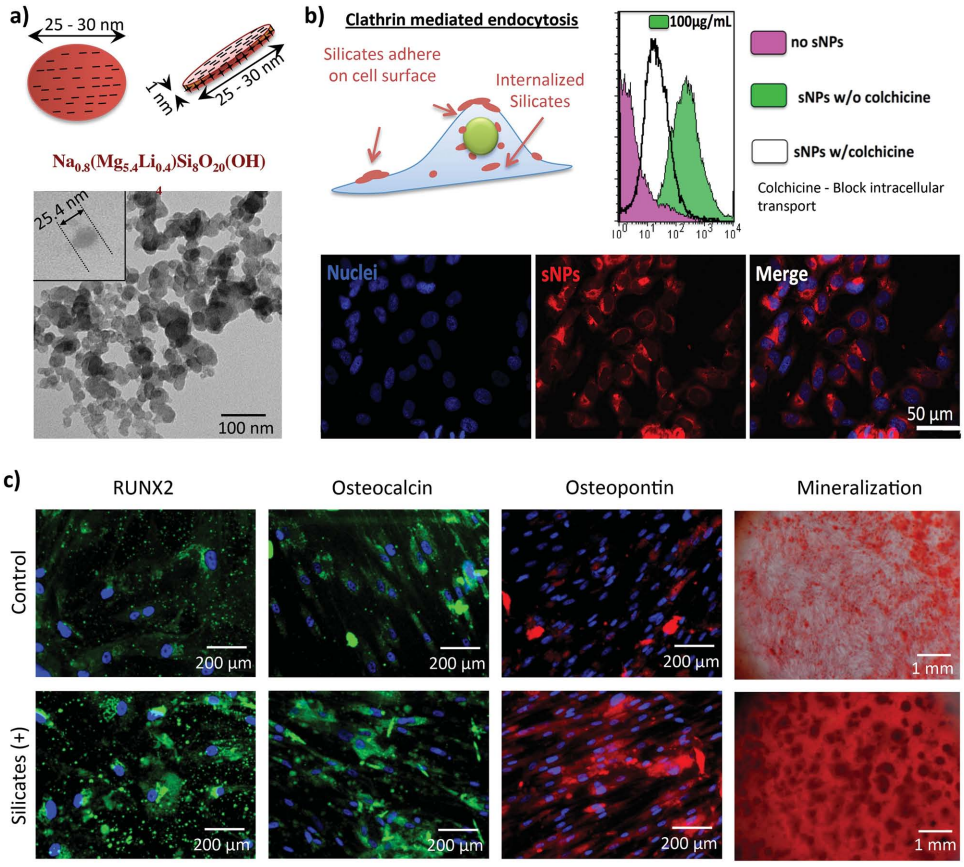

Figure 6. Nanosilicates could induce osteogenic differentiation of stem cells in the absence of osteogenic factors. a) Nanosilicates are disc shaped nanomaterials as obaserved from TEM images. b) Nanosilicates are internalized via clathrin-,mediated endocytosis. c) Nanosilicates were found to enhance expression of RUNX2, osteocalcin, osteopontin, and matrix mineralization of MSCs cultured in normal growth media. Reproduced with permission.[20,87] Copyright 2013, John Wiley & Sons, Inc. and 2014, Elsevier.

Halloysite (HAL) nanoclay ($Al_2Si_2O_5(OH)_4 \cdot 2H_2O$), an Al containing nanosilicates, was also shown to induce osteogenic differentiation of stem cells.[92] Nitya et al. reported that protein adsorption, mineral deposition, cell attachment, and spreading were higher on PCL/Halloysite nanosilicates (PCL/HAL) than on PCL nanofibrous scaffolds.[94] MSCs formed more organized actin cytoskeletons and stress fibers on PCL/HAL nanofibers. In addition, scaffolds with 4% HAL exhibited higher bioactivity and better cell responses compared to the ones with 6% HAL, perhaps due to the higher surface area of PCL/4%HAL from a smaller fiber diameter and exposed HAL. Similar to LAP-doped nanofibers, PCL/HAL nanofibrous scaffolds were found to induce osteogenic differentiation of MSCs in normal growth media.[94]

Another commonly used layered silicate is montmorillonite (MMT). Mieszawska et al. reported increased ALP activity, collagen type I, and bone sialoprotein in cells cultured on silk/MMT films in comparison to those cultured on silk/sodium silicate (control).[95] The amount of mineral nodules and surrounding fibrous structures also increased when MMT concentration increased from 0.65% to 1.4%. However, cell viability on silk/0.32% MMT was comparable to that on silk film and a TCP culture dish; the viability decreased considerably with higher MMT concentration. This could originate from a higher concentration of ionic moieties surrounding cells and poor solubility of MMT particles. Nanoparticles with limited solubility have been shown to induce inflammation and the release of ROS, leading to genotoxicity, which suggests further studies are needed to find optimal MMT concentrations, including a threshold value and minimum toxic concentration.[95]

Furthermore, Amber et al. mineralized hydroxyapatite on MMT clay to improve its osteoinductive properties, creating in situ hydroxyapatite-clay hybrids.[96] The hydroxyapatite-clay was then incorporated into chitosan/polygalacturonic acid (Chi/PgA) films by two methods: in method A, chitosan was mixed with polygalacturonic acid before being added to hydroxyapatite-clay; in method B, chitosan was first mixed with hydroxyapatite-clay and then added to polygalacturonic acid. It was found that the fabrication method had significant influence on seeded MSC behavior. For both A and B films, formation of mineralized nodules was observed in the absence of osteogenic growth factors, suggesting osteoinductive capabilities. However, for group B, MSC clusters floated, while for group A, they adhered on the films. Reasons for the formation of floating clusters were not clearly understood. One possibility was that on films prepared by method B, there were fewer in situ hydroxyapatite-clay sites available to interact with cells, due to in situ hydroxyapatite-clay mixed with chitosan before being

added to polygalacturonic acid. Also, after 14 days, some of the nodules started attaching to group B films, which might be attributed to increased exposure of in situ hydroxyapatite-clay. Nevertheless, this postulated reason was restricted to only 2D substrates. In addition, ALP activity was enhanced on group A films, compared to Chi/PgA films without in situ hydroxyapatite-clay (control). On the other hand, no significant difference was observed between group B films and controls. The underlying mechanisms need to be further investigated.[96]

4.4. Other Ceramic Nanoparticles

Ceramic nanoparticles can also be used as carriers for bioactive molecule delivery in tissue engineering. Liu et al. employed insulin-conjugated SiNPs for adipogenic differentiation of MSCs. Pure SiNPs were reported to have little cytotoxicity up to a concentration of 0.1 mg/mL, with no effects on osteogenic and adipogenic differentiation. After cultured in a medium with SiNPs-insulin, an abundance of lipid vacuoles were observed, indicating adipogenic differentiation. Notably, the amount of lipid vacuoles observed was comparable to that of when MSCs were cultured in a complete adipogenic differentiation medium with insulin. SiNPs were expected to assist in retaining bioactivity and stability of insulin. However, the advantages of using SiNPs as carriers over directly adding insulin to the culture medium need to be further illustrated.[97]

Once systematically available, owing to their small size, various nanomaterials can distribute to most organs in the body, and may cross biological barriers such as placental barriers and blood-brain barriers. Nevertheless, information regarding the ability of nanomaterials to cross the placental barriers and their developmental toxicity is scarce and inconsistent. Park et al. investigated developmental toxicity of SiNPs of different sizes (10, 30, 80, and 400 nm) by the embryonic stem cell test (EST). All SiNPs were uptaken and visible inside vacuoles of embryoid bodies. It was found that 80 and 400 nm SiNPs had no effect on metabolic activity and did not inhibit differentiation of D3 murine ESCs up to a concentration of 100 μg/mL. On the contrary, 10 and 30 nm SiNPs significantly decreased cell metabolic activity and appeared embryotoxic in a dose-dependent manner, as indicated by an inhibition of differentiation of D3 ESCs to cardiomyocytes. It was postulated that the observed results were related to the number of NPs taken up by cells; i.e., at equal concentration, there was a higher number of small NPs than that of bigger particles. The results could also be due to the higher surface area of small particles. Still, the reasons remain unclear. Notably, developmental toxicity occurred below cytotoxic concentration, raising a concern that systemic exposure to SiNPs would be harmful to embryos. Nevertheless, information regarding the ability of SiNPs to cross the placental barrier from mother to fetus is not yet established.[98]

In conclusion, various types of ceramic-based nanomaterials have been demonstrated to induce osteochondrogenic differentiation, suggesting their potential in hard tissue engineering. Osteoinductive nanomaterials such as nBGs and nanosilicates are promising alternatives to the use of a differentiation-inducing culture medium since inductive factors (e.g., dexamethasone, BMP-2) are relatively expensive and need to be newly added every time the medium is changed. Moreover, ceramic NPs can be used as drug/protein carriers because they are taken up by cells and capable of retaining the bioactivity of bioactive molecules. However, some results remain controversial and need to be further investigated—for example, the effects of nHA on the hydrophilicity of nanofibers and stem cell proliferation. It should also be noted that there are currently very few researchers focusing on the interactions of stem cells with nBG and nanosilicates, compared to those of nHA.

5. Carbon-Based Nanomaterials

Following the discovery of carbon nanotubes (CNTs) in the early 1990s, carbon-based nanomaterials have become a platform for biomedical engineering. Carbon-based nanomaterials (e.g., carbon nanotubes, fullerene, graphene, and nanodiamonds) have gained increasing interest owing to their biocompatibility and their unique structural, mechanical, thermal, and electrical properties. From an engineering perspective, another advantage is their ability to form different shapes and sizes with distinct properties. Among these materials, CNTs, graphene (G), and nanodiamonds (NDs) have been tested for tissue engineering applications. With increasing interest in carbon-based nanomaterials, there is a demand for an assessment of their potential hazards. While carbon is abundant in nature and bulk carbon materials are considered inert to cells, their reactivity increases drastically at the nanoscale. Specifically, carbon-based nanomaterials exhibit cytotoxicity with the general trend of CNTs > carbon black powders (CB) > NDs, from the most to the least cytotoxic. In this section, we discuss interactions of different types of carbon-based nanoparticles with stem cells and their cytotoxicity and genotoxicity.

5.1. Carbon Nanotubes

CNTs are ordered hallow tubes consisting of carbon atoms bonded to one another via sp^2 bonds, resulting in high mechanical strength and flexibility and thermal and electrical conductivity. Metallic single-walled carbon nanotubes (SWCNTs) can carry a current 50-fold greater than other metals.[99] Because of their tailored nanotopography and chemistry, incorporating CNTs into scaffolds leads to enhanced cell attachment, proliferation, and differentiation. For example, thin films of PEGylated, multi-walled carbon nanotubes (PEG-MWCNTs) support growth and induce osteogenic differentiation of MSCs without biochemical-inducing agents. In particular, in one study, an elongated fibroblast-like MSC morphology was observed on coverslips, PEG, and PEG-MWCNTs, whereas cells on carboxylated, multi-walled carbon nanotubes (COOH-MWCNTs) had irregular shape, suggesting poor adhesion and growth. Also, cell viability on coverslips, PEG, and PEG-MWCNTs were comparable, but significantly lower on COOH-MWCNTs.[100] This finding conforms to the study by Liu et al., where COOH-MWCNTs were found to inhibit proliferation and differentiation of MSCs.[101] Moreover, in the absence of BMP-2, cells on PEG-MWCNTs showed an elevated osteopontin (OPN), osteocalcin (OCN), and calcium deposition level after 14 days in

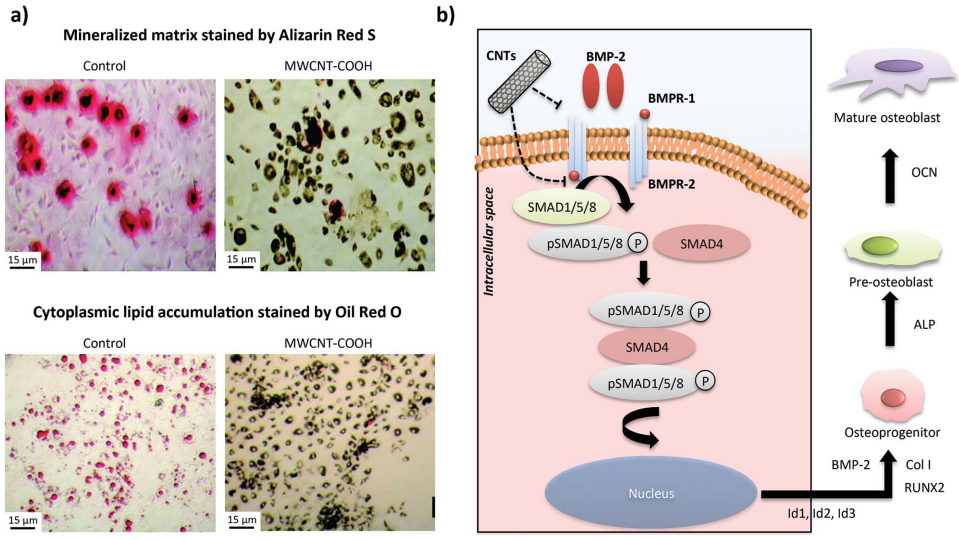

Figure 7. Effects of carbon nanotube functionalization on MSCs differentiation. a) MWCNT-PEG enhanced osteogenic differentiation as shown by Alizarin Red S staining. On the other hand, MWCNT-COOH inhibited both osteogenic and adipogenic differentiation. b) Plausible mechanisms of osteogenic differentiation inhibition by MWCNT-COOH. Reproduced with permission.[101] Copyright 2010, American Chemical Society.

culture. The result was indistinguishable from cells that underwent BMP-2 stimulation.[100] OCN is normally expressed after 21 days in osteogenesis, which is noteworthy. It was therefore hypothesized that PEG-MWCNTs served as an enhancer, accelerating the osteogenic differentiation processes. The discrepancies between PEG-MWCNTs and COOH-MWCNTs probably arose from different nanotopogrpahy; that is, PEG-MWCNT films were comparatively smoother. COOH-MWCNTs coated on coverslips were random, while PEG-MWCNTs created slightly parallel grooves and grids, which might be favorable for differentiation to bone lineage.[100]

Interactions between MSCs and COOH-CNTs were substantiated in the aforementioned study by Liu et al. Both carboxylated single-walled and multi-walled carbon nanotubes (COOH-SWCNTs and COOH-MWCNTs) in suspension exhibited cytotoxicity to MSCs, as evidenced by a decrease in cell viability even at the lowest dose (3 μg/mL).[101] Moreover, COOH-CNTs strongly inhibited both osteogenic and adipogenic differentiation (**Figure 7**). In particular, ALP activity was decreased in a time-dependent manner, without evidence of dose dependency. Formation of the mineralized matrix waned but in a dose-dependent fashion. Several osteogenic and adipogenic genes were down-regulated compared to controls. It should be noted that COOH-SWCNTs had slightly greater inhibitory effects than COOH-MWCNTs at all concentrations. Electron microscopy showed that some COOH-CNTs were taken up by MSCs and mainly localized in the perinuclear region and cytoplasm. However, most of them remained in the extracellular space; it was postulated that COOH-CNTs interacted with cell surface receptors or intracellular proteins, affecting signaling pathways, which led to inhibitory effects. Specifically, key proteins in the BMP-signaling pathway, such as Smad proteins and phosphorylated Smad proteins, were significantly reduced after COOH-CNTs treatments. In addition, ROS production and trapped metal impurities may have contributed to cytotoxicity of carbon-based nanomaterials. For example, pristine CNTs (p-CNTs) were shown to generate ROS-induced oxidative stress, which led to cell apoptosis via the NF-κB pathway. However, the results showed that no ROS was generated by COOH-CNTs, and Fe and Co present in p-CNTs were significantly reduced after strong acid treatments to produce COOH-CNTs. Thus, it was likely that the suppression of the BMP-signaling pathway down-regulated the osteogenic master transcription factor, Runx2, and consequently inhibited osteogenic differentiation. However, a number of adipogenic genes were down-regulated by COOH-CNTs; molecular mechanisms underlying these inhibitory effects need further investigation.[101]

On the contrary, Tay et al. reported that COOH-SWCNTs promoted cell adhesion, spreading, and neurogenic differentiation of MSCs in the absence of inducing factors but had no effect on osteogenic differentiation.[102] MSCs on COOH-SWCNTs were larger and more spread out than cells on coverslips due to differences in focal adhesions and cytoskeletons; particularly, stress fibers of cells on coverslips were more oriented and characterized by the presence of lamellipodia, whereas those on COOH-SWCNTs were relatively random and showed extensive formation of filopodia. These changes in cell morphology and cytoskeletons could be linked to enhanced neurogenic differentiation since extensive filopodia is a typical morphology of neurites. In addition, q-RT-PCR analysis showed that nestin and MAP-2, markers of neurogenesis, were upregulated on COOH-SWCNTs. Since filopodia has been proposed as a key sensory probe for nanotopography, it was believed that the topography of COOH-SWCNTs was the dominant factor inducing neurogenic differentiation, rather than chemical cues. However, this hypothesis has not been substantiated. Moreover, the discrepant results regarding cellular responses to COOH-CNTs between this and aforementioned studies remain inexplicable. Possibilities are differences in size/size distribution of CNTs and other uncontrolled factors during substrate preparation.[102]

Poly(acrylic acid) (PAA) is known to have negative effects on neuronal cell attachment and differentiation, primarily

due to the presence of carboxylic groups (COOHs), which have been extensively demonstrated to be negative cues for neuronal differentiation. A study by Chao et al. reported that PAA grafted on CNTs (PAA-g-CNTs) enhanced cell viability, adhesion, and neurogenic differentiation of ESCs.[22] The effects were even better than poly-L-ornithine (PLO), which is a conventional substratum for neuron culture; that is, neurogenic differentiation was two times greater on PAA-g-CNTs than on PLO. Also, differentiated neurons on PAA-g-CNTs had more branches, suggesting greater maturation of cells. PAA-g-CNTs were shown to have strong affinity to proteins, thereby enhancing cell attachment. These could be combinatorial effects of large specific surface areas and nanogrooves created by CNTs. Grafting polymers on CNTs could offer additional method to achieve selective differentiation of stem cells by combining topological cues from CNTs with biological cues from polymers. Although it is interesting to note that addition of CNTs can substantially change the cellular response to biomaterials, additional studies are need to fully elucidate the mechanism.

Furthermore, biocompatibility, mechanical strength, and especially electrical conductivity of CNTs make them excellent candidates for neural tissue engineering and neural interfaces since activities of neurons are highly electrical dependent. Current challenges in neuroprosthetic devices include delamination and degradation of metal electrodes, long-term inflammatory responses of surrounding tissues, miniaturization of electrodes limited by electrical properties of cell-electrode interfaces, and mechanical compliance with neural tissues that cannot be achieved by conventional semiconductors. In order to better integrate neural electrodes with surrounding neural tissues, Kam et al. created SWCNT-laminin composites in a layer-by-layer approach, aiming to humanize the materials by including ECM molecules. In comparison with laminin-coated glass slides, neuronal differentiation was more pronounced on SWCNT-laminin composites, as evidenced by longer neuronal outgrowths. In addition, a large amount of neurons and glial cells was observed on SWCNT-laminin composites with a strong presence of neurons, which suggested successful communication between differentiated cells and surrounding tissues. Synapsin between neurons and generation of action potential upon stimulation with a pulse signal further confirmed the formation of functional neuronal networks.[103] Although CNTs have shown positive roles in stem cell differentiation without inducing factors, long-term effects still need to be addressed. Concerns of their toxicity are discussed later in this Review.

5.1.1. Cytotoxicity and Genotoxicity of Carbon Nanotubes

It was reported that functionalization of MWCNTs with sodium sulfonic acid salt (e.g., $-SO_3Na$, –phenyl-SO_3Na) enhanced their biocompatibility with respect to unfunctionalized and COOH-functionalized nanotubes.[104] Similarly, functionalization of SWCNTs with –phenyl-SO_3Na, –phenyl-SO_3H, and -phenyl-$(COOH)_2$ was found to enhance biocompatibility. On the other hand, as previously mentioned, acid functionalization (e.g., –C = O, –COOH, –OH) of CNTs led to increased cytotoxicity. The disparities in cytotoxicity of unfunctionalized and functionalized CNTs may be attributed to dispersion, purity, and surface chemistry. For example, COOH-MWCNTs were more dispersed than MWCNTs, leading to a higher cellular internalization and hence enhanced cytotoxicity. On the other hand, strong acid treatments removed residual metal catalysts, amorphous, and other impurities from CNTs. Functionalization also changed the surface hydrophobicity, thereby preventing direct contact between CNTs and cells. These effects could mitigate cytotoxicity.[104]

In addition to cytotoxicity, genotoxicity studies pertaining to DNA damage and mutagenic effects are requisite. In many cases, genotoxic effects were found to occur below cytotoxic levels. For example, Lindberg et al. reported that CNTs and graphite nanofibers (GNFs) appeared genotoxic to human bronchial epithelial cells at doses that were not overly cytotoxic.[105] Both of them induced DNA damage in a dose-dependent manner, with CNTs having a slightly higher degree of genotoxicity. Moreover, CNTs and GNFs increased micronucleated cells, but independent of dose. The lack of dose-dependent effects in micronuclei assay could be attributed to an increasing size of agglomerates at a higher dose, prohibiting cellular uptake. Moreover, cells were partly covered by agglomerated nanomaterials, making analysis more difficult. The fact that dose dependency was observed in a comet assay (for DNA damage) but not a micronuclei assay could be due to different study endpoints, higher sensitivity of the comet assay, and aforementioned technical limitations. Previous studies suggested that MWCNTs could induce micronuclei formation by either aneugenic and/or clastogenic mechanisms, yet the details remain unknown. In addition, whether residual metal catalysts contribute to genotoxicity of CNTs is contentious. Muller et al. reported that MWCTs did not generate ROS but instead showed radical scavenging capacity, while other studies presented the opposite trend.[104] It was reported that ESCs expressed higher levels of p53 proteins after 2 hours of exposure to MWCNTs, and the level seemed to correlate with MWCNT dose. Since p53 activates cell cycle checkpoints and generally remains at low levels in normal conditions, the enhanced p53 expression was an indication of DNA damage. Further studies suggested that MWCNTs induced DNA damage by a mutagenic guanine base lesion, which could cause subsequent breakage of DNA double strands. These modifications can bring about various mutations, such as point mutations, mitotic recombination, and chromosome loss and translocation. Accordingly, MWCNTs were found to increase mutation frequency two-fold in ESCs. These results suggest p53 expression levels as an early indicator to assess genotoxicity of nanomaterials.

5.2. Graphene and Graphene Oxide

Graphene (G) is an atom-thick monolayer of carbon atoms arranged in a honeycomb lattice. Compared to CNTs, graphene presents open surfaces for non-covalent interactions with biomolecules. Although graphene is a building block of CNTs, research on its potential in tissue engineering has been at a nascent stage since an initial report in 2004.[5,106] Interestingly, graphene is reported to have a higher Young's modulus (0.5–1 TPa) than any known material, yet it is not brittle. As a result, it can

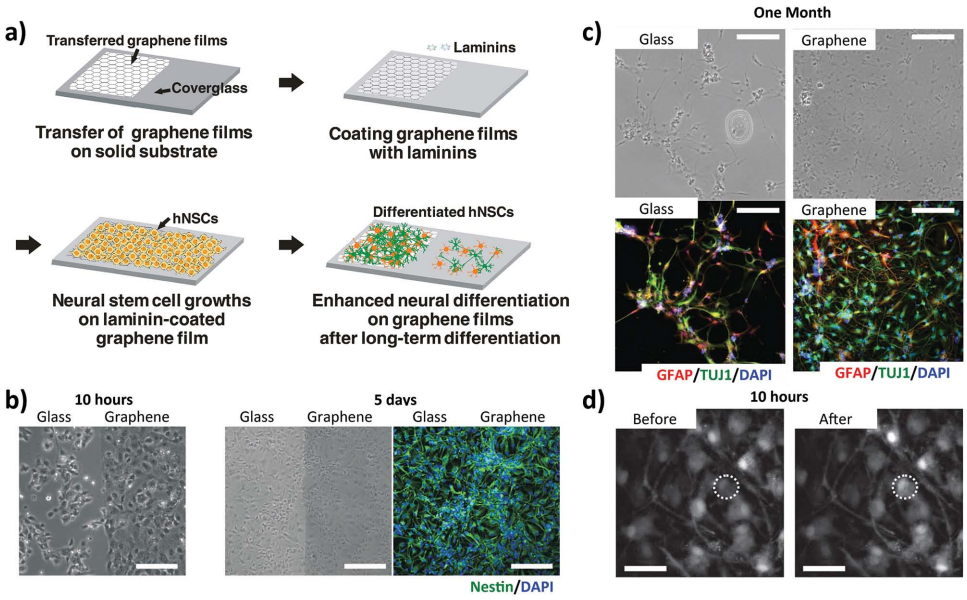

Figure 8. Surface functionalization of graphene with laminin. a) promotes neural stem cell adhesion and its differentiation into neurons. b) hNSCs prefer to grow on graphene compared to glass surface. c) Enhanced neural-differentiation of hNSCs on graphene films as evident by TUJ staining. d) Calcium imaging of the differentiated cells on graphene before (left) and after (right) electrical stimulation. Reproduced with permission[108] Copyright 2011, Elsevier.

be transferred onto any surface, creating a strong yet flexible substrate.

Owing to this unique set of properties, it is a good candidate for bone tissue engineering. For example, Nayak et al. reported that graphene accelerated osteogenic differentiation of hMSCs. While osteogenic media alone was insufficient to induce osteogenic differentiation on uncoated substrates, graphene coating significantly enhanced OCN expression and calcium deposition regardless of underlying materials.[107] Particularly, besides glass slides, the effects were also observed on softer substrates (i.e., polydimethylsiloxane (PDMS) and polyethylene terephthalate (PET)), whose stiffness does not promote bone formation. A parallel study further showed that graphene-coated PET could induce osteogenic differentiation in the absence of BMP-2. Although graphene coating and BMP-2 treatment induce cell differentiation at the same rate, BMP-2 needs to be administered every 3 days due to a short half-life, thereby suggesting graphene as a potential replacement of BMP-2. These effects were probably attributed to the ability of graphene to sustain lateral stress such that it created the right amount of cytoskeletal tension. Such tension might subsequently change conformation of mechanically sensitive proteins of interest.[107]

Additionally, graphene was shown to enhance the differentiation of NSCs to neurons without neurogenic inductive factors. Park et al. reported that cells on both graphene and glass substrates exhibited neurite outgrowths (**Figure 8**).[108] However, during differentiation processes, cells on glass aggregated and started to detach, whereas the ones on graphene adhered solidly, suggesting that graphene provided a more favorable microenvironment. The differentiated cells on both substrates consisted of neurons and glia, but the percentage of neurons was significantly higher on graphene. It was found that laminin-related receptors of cells on graphene were upregulated, which explained the enhanced cell adhesion. In addition, it was previously shown that NSCs preferentially differentiated to neurons rather than glia when surrounded by a large number of glia. In this study, with more cells in total on graphene during differentiation processes, it was likely that NSCs on graphene were surrounded by a larger number of glia compared to those on glass. As a result, the percentage of neurons was higher on graphene substrates. Moreover, graphene films exhibited electrical coupling with differentiated neurons, suggesting an application for neural stimulating electrodes in treating brain diseases.[108]

Graphene's derivative, graphene oxide (GO), has garnered equal interest. Chen et al. conducted a comparative study of behaviors of iPSCs on G, GO, and glass surfaces.[109] It was found that cell adhesion and proliferation on G and glass were comparable but lower than those on GO. Moreover, G favorably maintained stemness of iPSCs, while GO on glass expedited differentiation. The tendency of iPSCs to differentiate in three germ layers varied on G and GO. In particular, iPSCs on G and GO spontaneously differentiated along ectodermal and mesodermal pathways without significant disparity; on the other hand, endodermal differentiation was suppressed on G while augmented on GO. These findings could be useful for maintaining pluripotency of iPSCs without feeder layer cells and guiding differentiation toward specific lineages. Considering the different abundance of polar groups and hydrophilicity for G and GO, and the fact that certain functional groups such as the aforementioned carboxylic group significantly affected stem cell differentiation, it was possible that differences in surface groups might affect types of cell surface receptors bound to G and GO. Consequently, signaling transduction pathways were differentially regulated, leading to disparities in differentiation propensity. Nonetheless, surface molecules and signaling pathways of iPSCs were not as well understood as those of ESCs

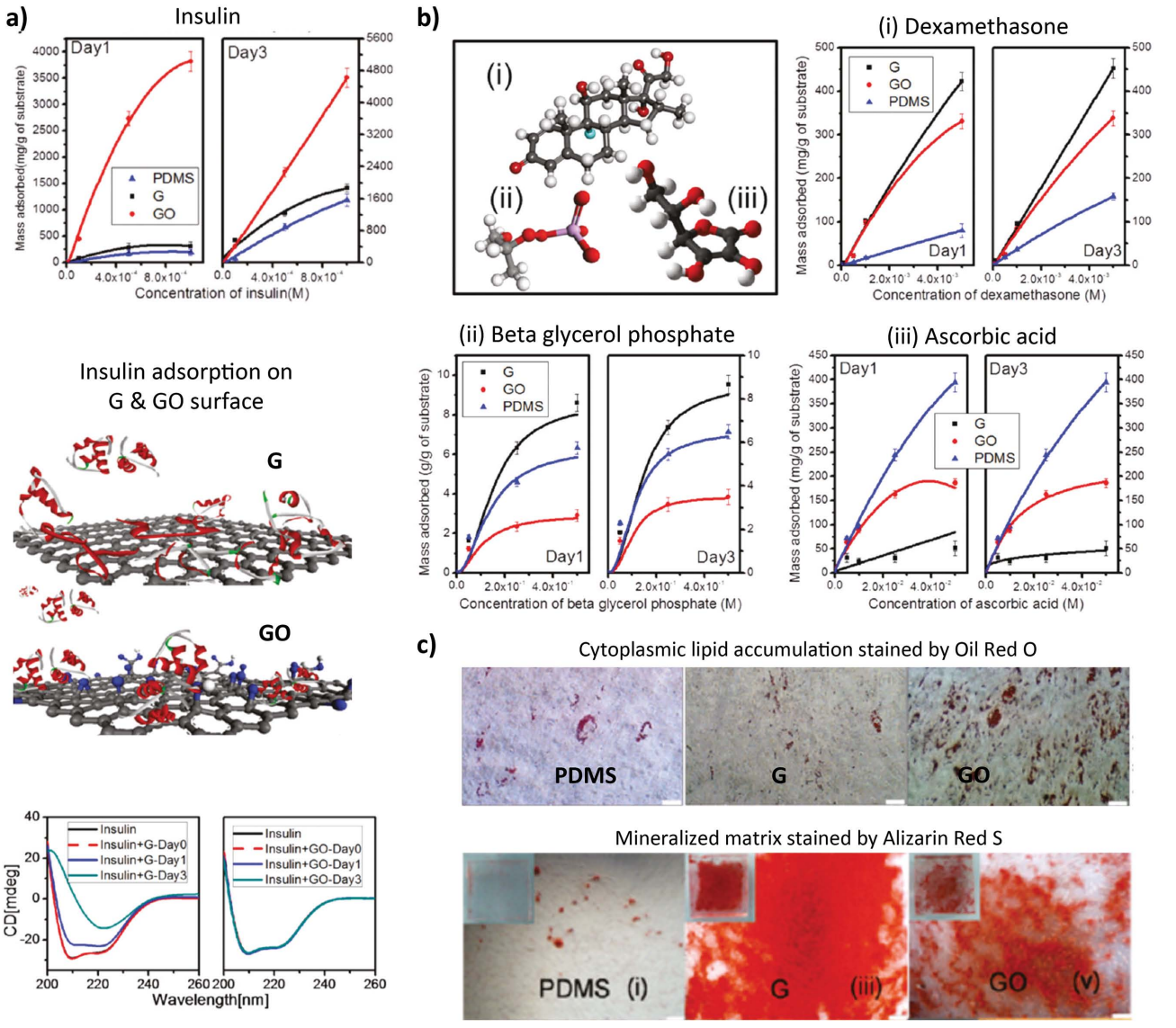

Figure 9. MSCs differentiation on graphene (G) and graphene oxide (GO). a) Insulin was adsorbed more on GO than G, whereas osteogenic factors were adsorbed more on G. b) Schematic of dexamethasone (i), beta glycero phosphate (ii), and ascorbic acid (iii). High adsorption capacity of G for dexamethasone could be attributed to π–π interactions between benzene rings of dexamethasone and the substrate. c) Consequently, osteogenic differentiation was enhanced on G while adipogenic differentiation was enhanced on GO. Reproduced with permission.[106] Copyright 2011, American Chemical Society.

or MSCs; thus, underlying mechanisms need to be further studied.[109]

Recently, Lee et al. investigated the origin of enhanced growth and differentiation of MSCs on G and GO.[106] They observed that more proteins were adsorbed on GO than G, and both were significantly greater than on PDMS control. Although PDMS and G had similar hydrophobicity, τ-electron clouds in G enabled interactions with a hydrophobic core of proteins and drug (**Figure 9**). Greater protein adsorption on GO was mainly attributed to the presence of oxygenate groups (i.e., epoxide, carboxyl, or hydroxyl), which facilitated protein binding via covalent, electrostatic, and hydrogen bonds. In addition, osteogenic differentiation was enhanced more on G than GO, as evidenced by more mineral deposition under chemical induction. It was found that G absorbed a higher amount of Dex and β-glycerolphosphate (Figure 9a &b). That is, G was able to pre-concentrate osteogenic inducers, which was attributed to π–π stacking between aromatic rings of biomolecules and the basal plane of G. Because GO possesses a higher density of oxygenated groups, it experienced larger electrostatic repulsion from phosphate ions. On the other hand, G adsorbed less ascorbic acid since it had no available groups to form hydrogen bonds with acids. However, this did not abate osteogenic differentiation on G since ascorbic acid is known to affect only mature osteoblasts. Based on the fact that extensive mineralization was observed only when cells were cultured in osteogenic media, it is likely that the ability of G to pre-concentrate inductive agents was a key factor inducing differentiation rather than the

corrugated topography of G. Moreover, adipogenic differentiation was enhanced on GO while suppressed on G (Figure 9c). Accordingly, GO exhibited over a two-fold higher insulin (main mediator for fatty acid synthesis) adsorption than G, which was attributed to electrostatic interactions and hydrogen bonding between GO and proteins, which maintained a three-dimensional conformation of insulin (Figure 9c). On the contrary, adsorbed insulin on G was denatured as a result of strong π–π stacking on G.[106]

In a recent study, Tatavarty et al. observed that the osteogenic activity of GO could be enhanced by designing nanocomposites from GO and calcium phosphate nanoparticles.[110] They synthesized pluronic® F127 coated GO–CaP and CaP using a double-reverse microemulsion method. Stem cells readily adhere on these nanocomposite materials and showed significantly higher production of mineralized matrix on GO-CaP nanocomposite compared to GO and CaP. The immunofluorescence staining of osteoblast markers alkaline phosphatase (ALP) and osteocalcin (OCN) were also upregulated on GO-CaP compared to CaP and GO. Although the exact mechanism of osteogenic activity of GO is still not know, but it is believed that some of the properties of GO such as nanotopography, high stiffness, electrical conductivity and ability to adsorption protein might control the fate of stem cells.[111]

Nanotopography could be introduced to GO to further enhance stem cell differentiation. Akhavan et al. created reduced graphene oxide nanoribbons (rGONR) on a SiO_2 substrate containing TiO_2 NPs and applied a photocatalytic stimulator to accelerate neurogenic differentiation of NSCs.[112] They observed that cells were more differentiated on rGONR compared to those on rGO sheets and quartz substrates, which was attributed to physical stress induced by nanotopography. The neuron-to-glia ratio was also the highest on rGONR. In addition, flash photo stimulation, which created electric fields along nanogrids, could further induce elongation of differentiated cells and an increased number of neurons.[112]

5.2.1. Cytotoxicity and Genotoxicity of Graphene and Graphene Oxide

Graphene also showed concentration-dependent cytotoxicity. It was found to reduce cell adhesion, enter into various cell compartments, and eventually induce apoptosis. Most studies to date have reported reduced or negligible cytotoxicity for graphene oxide. In fact, there are many factors influencing cytotoxicity of graphene and its derivatives, such as concentration, size, shape, dispersants, and especially functionalization.[5] Similar to CNTs, cytotoxicity of graphene can be tuned by functionalization. For example, pristine graphene was found to aggregate on Vero (monkey kidney cells) cell membranes as a result of strong hydrophobic interactions between pristine graphene and lipid membranes. This led to membrane deformation and destabilization of F-actin alignment and, eventually, apoptosis. The programmed cell death was not attributed to membrane damage or leakage of cytoplasmic enzymes but rather ROS. It was postulated that accumulation of pristine graphene on cell membranes might impede nutrient and protein uptake, as well as obstruct ion channels, leading to internal stress. In contrast, more hydrophilic carboxyl functionalized graphene was found to be internalized without affecting cell morphology. In particular, carboxyl functionalized graphene had negligible effects on cell viability up to the highest concentration tested, 300 μg/mL.[113] Biocompatibilty of graphene oxide could also be improved by functionalization with PEG or dextran. Nevertheless, cytotoxicity of pristine graphene itself might not be pertinent to tissue engineering, for which it will need to be functionalized before any potential use. The more pivotal question is how to modify graphene such that cytotoxicity is minimized.[5]

Shape and size of graphene materials were shown to significantly affect how they interacted with stem cells. Akhavan et al. reported that reduced graphene oxide nanoribbons (rGONRs) had higher cytotoxicity than reduced graphene oxide sheets (rGOSs).[114] Both of them reduced viability of MSCs in a dose- and time-dependent manner, with a threshold concentration of 10 and 100 μg/mL for rGONRs and rGOSs, respectively. The cytotoxic effects of graphene oxide sheets (GOSs) were similar to those of rGOSs but with lower cytotoxicity. Similarly, graphene oxide nanoribbons (GONRs) were found to have lower toxicity than rGONRs. Mechanisms involved in cytotoxicity of rGONRs and rGOSs were ROS generation and damaging cell membranes via direct contact with sharp edges of graphene. Specifically, ROS-induced oxidative stress played a key role in rGOSs cytotoxicity, whereas membrane damage as evidenced by RNA effluxes was more pronounced for rGONRs than in rGOSs. This could be attributed to sharper edges and higher mobility of rGONRs.[112] In addition, reduced graphene oxide nanoplatelets (rGONPs) with an average lateral dimension (ALD) of 11 ± 4 nm caused substantial cell destruction at 1.0 μg/mL, compared to rGOSs with an ALD of 3.8 ± 0.4 μm, which exhibited cytotoxicity at 100 μg/mL. Accordingly, ROS generated by rGONPs was two-fold higher than that generated by rGOSs due to additional edge defects presented by rGONPs serving as active sites for ROS production. Similar to rGONRs, damaging cell membranes was another mechanism involved in rGONPs' cytotoxicity. However, neither ROS generation nor cell membrane damage could explain cell destruction at a low concentration (1.0 μg/mL) of rGONRs and rGONPs, a concentration at which substantial changes in cell morphology and apoptosis were not observed.[114]

Previous observations found genotoxicity responsible when neither ROS generation nor cell membrane damage could explain cytotoxicity at low concentrations of rGONRs. DNA fragmentation and chromosomal aberrations in MSCs were observed after exposure to rGONRs in a dose- and time-dependent manner. This occurred at a concentration of 1.0 μg/mL, one order of magnitude lower than the cytotoxic threshold (10 μg/mL).[112] Because RNA efflux was not detected at this concentration, genotoxicity of rGONRs was mainly attributed to penetration of rGONRs into cells, which was promoted by their sharp edges and high motility.[112] Similarly, rGONPs initiated DNA fragmentation and chromosomal aberrations at a concentration of 1.0 μg/mL. On the other hand, rGOSs induced slight DNA fragmentation and no chromosomal aberrations at concentrations greater than 100 μg/mL. These results demonstrate the effects of shape and size of graphene materials on their interactions with stem cells. They also emphasize the

significance of genotoxicity assessment that typically occurs below cytotoxic levels.[114]

5.3. Nanodiamonds

Magnetic properties and strong near-infrared (NIR) photoluminescence make nanodiamonds promising alternatives to current imaging platforms. However, there is limited research on applications of NDs in tissue engineering with stem cells. One study by Xing et al. reported that ESCs treated with oxidized nanodiamonds (O-NDs) exhibited reduced ALP activity and increased Oct-4 expression, whereas pristine/raw nanodiamonds (P-NDs) generated the opposite response.[115] The authors concluded that O-NDs induced differentiation, while P-NDs maintained ESC stemness. Interestingly, embryonic stem cells expressed high amounts of ALP early on, which waned as they began to differentiate, until the cells decided to go down to the specific osteoblastic lineage, where they began expressing ALP again.[115]

5.3.1. Cytotoxicity and Genotoxicity of Nanodiamonds

Nanodiamonds have relatively lower cytotoxicity compared to other carbon-based nanomaterials and have been shown to be well tolerated by various cell types. In particular, in one study, cells maintained high viability after being incubated with NDs for several days. Also, NDs did not elicit ROS-induced oxidative stress. Despite low toxicity, NDs were found to alter cell morphology. For example, neuroblastoma cells treated with NDs displayed distinct branching and neurite extension with respect to controls. However, it is currently unknown whether NDs bonded directly to actin cytoskeletons or affected certain signaling pathways. The previously stated biocompatibility trend (NDs > CB > MWCNTs > SWCNTs) was found to agree with the amount of ROS generated by each material (i.e., SWCNTs > MWCNTs > CB > NDs). Increased ROS production could be attributed to residual metal catalysts (e.g., Fe, Ni, Co) used in material synthesis since they followed the same trend. The amount of Fe extracted from MWCNTs and SWCNTs was reported to be 0.49wt% and 0.26wt%, respectively, compared to undetectable levels for CB and NDs.[104]

NDs have been shown to have lower genotoxicity than other carbon-based nanomaterials. Xing et al. reported that P-NDs and O-NDs induced DNA damages in ESCs, as evidenced by slight increases in the DNA repair protein, p53.[115] Expression of MOGG-1, another DNA repair protein, was also enhanced by O-NDs but not P-NDs. For both NDs, p53 expression was higher at a low dose (5 μg/mL) compared to a high dose (100 μg/mL), which could be attributed to aggregation of NDs at high doses. Specifically, since the solubility of NDs in the culture medium was limited, the number and size of aggregates increased with increasing concentration. Consequently, they stuck onto cell membranes rather than entered cells. Some of the small NDs were internalized but primarily remained in the cytoplasm with negligible nuclear entry. Despite enhanced p53 levels, no obvious structure damages by P-NDs were observed, suggesting that the damage was minor and could be repaired shortly thereafter. In addition, O-NDs appeared to be more cyto- and genotoxic than P-NDs. That is, O-NDs were found to cause more DNA damage and induced apoptosis by the uptake of small particles. More profound genotoxicity of O-NDs could originate from different surface chemistry. Increased O-ND solubility could be another possibility leading to less aggregated and more internalized particles. Since NDs at high concentrations spontaneously form clusters that are often too big to pass through nuclear pores, it is likely that DNA damage was brought about by indirect mechanisms that remain to be further investigated.[115]

Owing to their biocompatibility and unique structural, mechanical, thermal, and electrical properties, carbon-based nanomaterials have shown promising potential in biomedical applications, especially in bone and neural tissue engineering. Also, functionalization of these materials creates distinguished effects on material–stem cell interactions. Because they are nonbiodegradable and highly reactive, there is a pressing demand for assessment of their cytotoxicity and genotoxicity. At their nascent stage, there is some controversy pertaining to interactions between stem cells and carbon-based nanomaterials, such as the underlying mechanisms of observed cell destruction and DNA damages. From the works reviewed, it is apparent that there is plenty of room for further research.

6. Metal/Metal-Oxide Nanomaterials

Currently, there is widespread commercial use of metallic nanomaterials, most notably nanosilver (Ag), in a diverse group of fields. Known for its antimicrobial effects, nanosilver has been considered for a variety of medical applications. Other metal nanomaterials have also emerged for use in medical imaging or as modified substrates for tissue engineering systems. Their atomic composition allows for some unique properties when, for example, placed within a magnetic field or stimulated electrically, and these characteristics coupled with nanoscale size lead to some very exciting possibilities. For example, nanoscale topography combined with growth factors can be used to control stem cell fate in a synergistic (Figure 10).[116] As the interest in these metallic nanomaterials has grown, investigations into biological interactions between the materials and human cells have also increased in popularity. Stimulation events at the cellular membrane as well as internalization of metallic nanomaterials engage a diverse array of transduction pathways within the cell, further motivating cell behavior. In some instances, the consequences following metallic nanomaterial introduction can be detrimental to the cell. Therefore to better characterize these types of materials, new nanomaterials have been introduced in a variety of tissue engineering applications, introducing the need to specifically uncover biocompatibility and bioactivity with stem cells.

6.1. Silver Nanoparticles

6.1.1. Silver Nanoparticle Cytotoxicity

A variety of metal oxide nanotube arrays, gold NPs, and superparamagnetic iron oxide nanoparticles (SPION) have been

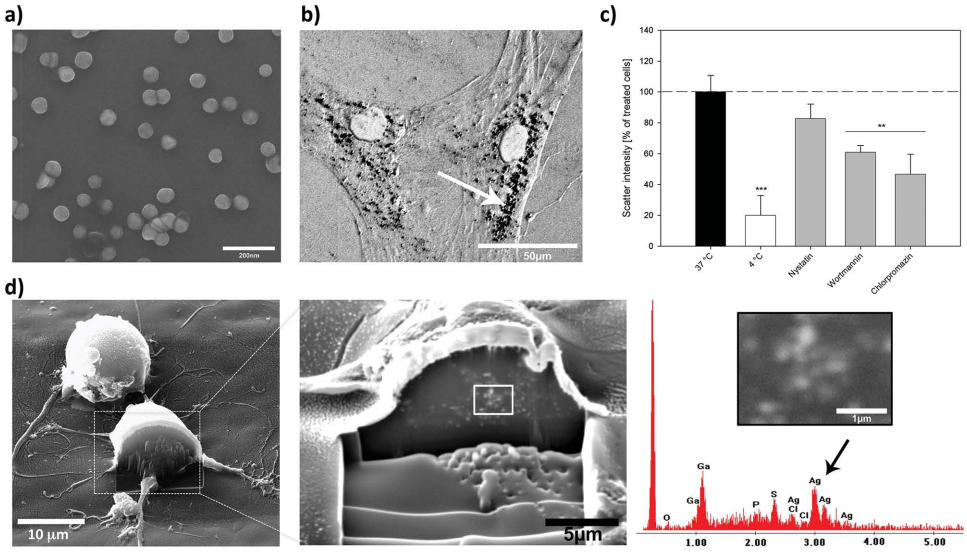

Figure 11. Ag nanoparticles-MSCs interactions. a) SEM images of PVP-coated Au nanoparticles. b) nanoparticles are easily internalized within cell body as determined cia TEM imaging. c) Ag nanoparticles are uptake primiraly via clathrin-mediated (chlorpromazin) and macropinocytosis-mediated (wortmannin) pathway. d) Detection of Ag-NP within cells was determined via EDX spectra of milled cell. Reproduced with permission.[119] Copyright 2011, Elsevier.

used in tissue engineering systems; however, due to its commercial availability, nanosilver is one of the more highly studied metallic nanomaterials. Kittler et al. synthesized Ag-NPs stabilized with polyvinylpyrrolidone (PVP) and monitored bioactivity of hMSCs.[117] The 100 nm particles were compared to free silver ions, and both demonstrated concentration-dependent cytotoxicity. While the free ions showed a significant decrease in viability at a concentration of 2.5 μg /mL, the coated NPs were not cytotoxic until a concentration of 5 μg/mL. Both concentrations exceeded that of reported cytotoxic concentrations for microbial systems.[118] They also observed that PVA coated Ag-NPs easily internalized within MSC (**Figure 11**a,b).[119] The same group found that the chemotaxis of hMSCs was significantly reduced around 3.5 μg/mL for PVP-Ag-NPs, with Ag ions again reducing function at 2.5 μg/mL.[117] Cytokine release of hMSCs was also shown to follow similar dose-dependent trends. Interestingly, cytokine IL-8 showed a significant increase in its release at a non-toxic NP concentration of 2.5 μg/mL, which could act as a kind of cellular alarm. This response may not be limited to Ag, considering a similar result was found with nickel ions and hMSCs in vitro. While the mechanism for this result has yet to be elucidated, it uncovers an interesting aspect of cellular behavior in response to metallic nanomaterials.[117] A later study found a similar increase in IL-8 at non-toxic NP levels; however, researchers also saw a similar trend with IL-6 and VEGF. While the results are not in complete agreement with Greulich et al. (2009), they provide more evidence of hMSC activation at subtoxic silver NP levels. Some of the variability could be attributed to the differences in particle size, considering the particles used were 50% smaller, as well as to the surface chemistry (no coating was utilized for the Ag-NPs). Hackenberg et al. likewise monitored DNA damage within hMSCs at varying silver NP concentrations and found DNA fragmentation significantly increased at concentrations of 0.1 μg/mL and greater for all exposure times examined. A similar trend and concentration threshold was observed for chromosomal aberrations in 50 metaphase cells. Again, the mechanism for the resulting DNA damage has yet to be fully explained.[120]

Some researchers have taken the next step to better understand the processes of cytotoxicity and genotoxicity by characterizing the intracellular uptake and distribution of Ag-NPs. To determine the endocytic pathway responsible for the internalization of 80 nm Ag-NPs, Greulich et al. (2011) pre-treated hMSCs with three inhibitors (35 μM chloropromazine hydrochloride, 10 μM nystatin, or 400 nm wortmannin) and then exposed the cells to PVP-coated Ag-NPs (Figure 11c).[119] These treatments are responsible for inhibiting clathrin-mediated endocytosis, caveolae-specific endocytosis, or macropinocytosis, respectively. Flow cytometry analysis of each group showed that while clathrin-mediated endocytosis was the most effective treatment in limiting uptake, it was not the only mechanism within the cell. Macropinocytosis was also partly responsible for the accumulation of NPs within the cell. Upon internalization, particle agglomerates were observed in the perinuclear region by EDX spectra of ion-milled cells (Figure 11d) as well as fluorescent micrographs. The particles were distributed through endo-lysosomal areas, and the amount corresponded to NP concentration. Entrance into other cellular compartments was not observed, which was hypothesized to be due to the larger size of the agglomerates within the endocytic vesicles. Future work is still needed to confirm these pathways of internalization as well as determine their relevance for other metallic biomaterials.[119]

Once NPs are internalized, cells generation ROS causing oxidative stress and eventually cell death if ROS is significantly higher.[120–122] Ag^+ ions released from Ag-NPs within endocytic vesicles or from NP surface interactions with cellular proteins could negatively affect the mitochondrial respiratory chain by disrupting the electron transport chain (**Figure 12**a,b).[121] An increase in ROS and a decrease in metabolic activity could be

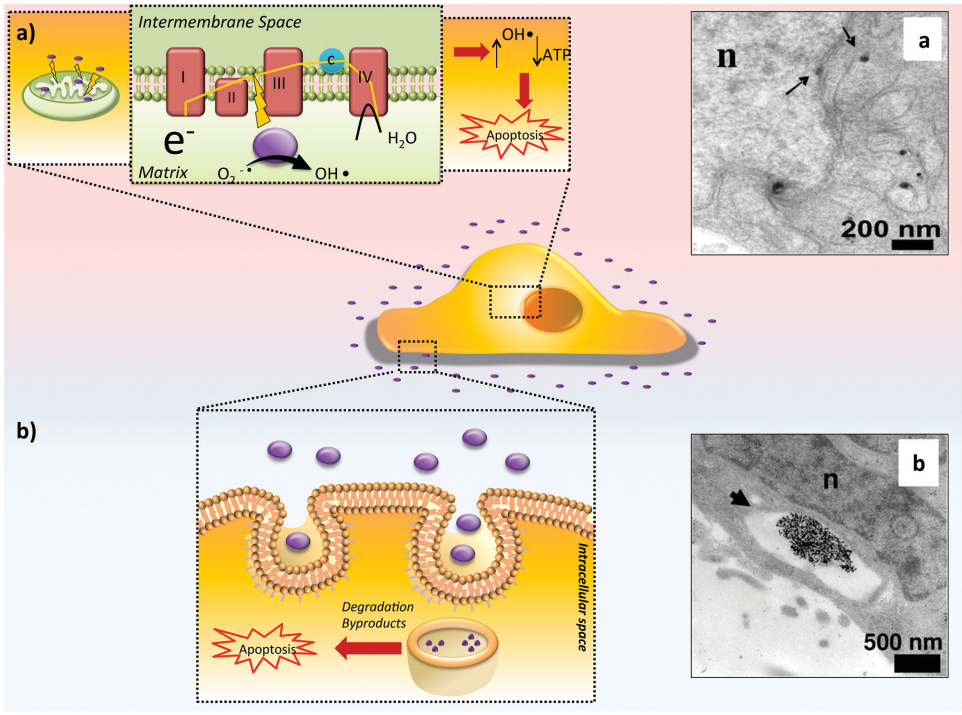

Figure 12. Interaction of metal ions release from AgNPs with stem cells. a) Metal nanoparticles are endocytosed via vesicle transport, escape, and interfere with mitochondrial function through disruption of electron transport chain, generating superoxide anions ($O_2^{-\bullet}$), reducing transition metals eventually leading to hydroxyl radicals or peroxynitrite, which can react with proteins and DNA. ATP synthesis is also decreased, which in combination with radical production, can lead to cell death. Arrows in electron micrographs indicate accumulated nanoparticles in mitochondria as well as on nuclear membrane; b) Internalization of nanoparticles into low pH environments within intracellular vehicles may result in release of cytotoxic degradation byproducts into the cytosol, impairing cellular function and likewise lead to cell death. Electron micrograph displays an endosome containing accumulated nanoparticles for transportation. Adapted and reproduced with permission.[121] Copyright 2009, American Chemical Society.

responsible for the observed cytotoxic and genotoxic effects in vitro. The DNA damage in human lung fibroblast cells (IMR-90) and human glioblastoma cells (U251) by measuring cell cycle arrest and found that an increased number of cells accumulated in the gap$_2$/mitosis (G_2/M) phase as the concentration of applied NPs increased. Comet assay and cytokinesis-block micronucleus assay correlated with their cell cycle findings. Due to the significantly greater NP concentrations applied (up to 400 µg/mL) and the usage of differentiated cells, the work left questions as to stem-cell-specific interactions at cytotoxic concentrations previously reported; however, it would be safe to hypothesize a similar mechanism is behind the toxicity of these NPs in stem cells.[121]

6.1.2. Silver Nanoparticles Influences on Cellular Differentiation

A final consideration of Ag-NPs applied to stem cells is their effect on differentiation. For TE applications, differentiation into a fully functional cell type is a primary concern. If this process is discouraged or inhibited by a biomaterial utilized in the system, there will be a fundamental flaw in the design. Therefore, our knowledge of the induction capabilities of these materials must be comprehensive. Unfortunately for Ag-NPs, there is not a consensus of opinion on their effect on differentiation. For example, Park et al. (2011) reported that murine embryonic stem cells showed a decrease in differentiation capacity both dose specific and size specific, with a 20 nm particle demonstrating the most potency, and noted that this effect was observed at concentrations similar to or greater than those decreasing metabolic activity, which could indicate an indirect cause from cytotoxicity and not a direct interaction with the nanoparticle.[122] Opposingly, Samberg et al. found no evidence supporting the notion that Ag-NPs disrupt human adipose-derived stem cell (hASC) differentiation after exposure to either 10 or 20 nm NPs at any concentration tested.[123] They also reported no significant cytotoxicity to hASCs, which differs from previous cytotoxicity studies with hMSCs. They suggested that the variability on reported toxicity stems from a difference in synthesis method, NP washing, or duration of particle storage. The discrepancies in results illustrate the need for a comprehensive toxicity study in which Ag-NP preparation and application are varied for a more complete toxicity profile.[123]

6.2. Gold Nanoparticles

Due to their usefulness as conductive materials as well as being biocompatible, gold-based nanomaterials have the potential for use in biomedical applications. Recently, gold nanomaterials have emerged as a vehicle for electrical stimulation for cellular induction. By coating a surface with these nanoparticles, researchers can create a thin film capable of conveying an electrical event, which can then be functionalized for effective cell

seeding.[124] In one study, human embryonic stem cells (hESCs) that had been transfected with an Oct-4-promoter conjugated with enhanced green fluorescent protein (EGFP) via lentiviral vector were monitored after seeding on a PEI pre-coated layer with an Au NP/fibronectin monolayer on top. The Oct-4 gene expression was monitored via cell sorting and fluorescence microscopy.[124] Prior to differentiation, more than 70% of undifferentiated hESCs were positive for a high expression of Oct-4, which suggested the gene was relevant for pluripotency maintenance. After electrical stimulation, gene markers were targeted to uncover induction into a specific germ lineage. The most robust change in expression occurred with the mesoderm lineage marker T-gene. RT-PCR further corroborated mesodermal lineage differentiation. While the efficiency of the differentiation process was not provided, nor was a hypothesis offered as to why, for example, the experiment parameters led to the formation of mesoderm lineage as opposed to nervous tissue (ectoderm), the study demonstrated a technique with potential to address some of the issues associated with differentiation in TE applications.[124]

Another group took a second approach toward the differentiation of stem cells using Au-NPs. They synthesized Au-NPs ≈20nm in diameter and observed that MSCs easily internalized the nanoparticles (**Figure 13**a,b) Cultured MSCs received varying concentrations of Au-NPs, which led to varying success of osteogenic differentiation.[125] At higher concentrations, the cells showed improved differentiation, seen by higher ALP activity as well as mineralization through an Alizarin Red S stain. Microscopy provided evidence of morphological changes suggestive of osteogenic differentiation (well-spread, polygonal morphology). Concurrently, the NPs showed inhibition of adipogenic differentiation in the presence of an adipogenic supplement, which was monitored by oil red O staining. RT-PCR analysis of osteogenic and adipogenic gene expression illustrated the same trends since Runx2, ALPL, and BMP-2 expression all increased, while adipogenic-specific PPARγ expression decreased (Figure 13c). The p38 mitogen-activated protein kinase (MAPK) pathway was also upregulated, which researchers suspected was caused by mechanical stress associated with subsequent binding of NPs to proteins after endocytosis and which led to the enhanced expression of osteogenic genes. A next step would be to uncover the endocytic entrance pathway to further clarify this mechanism of MAPK stimulation (Figure 13d).[125]

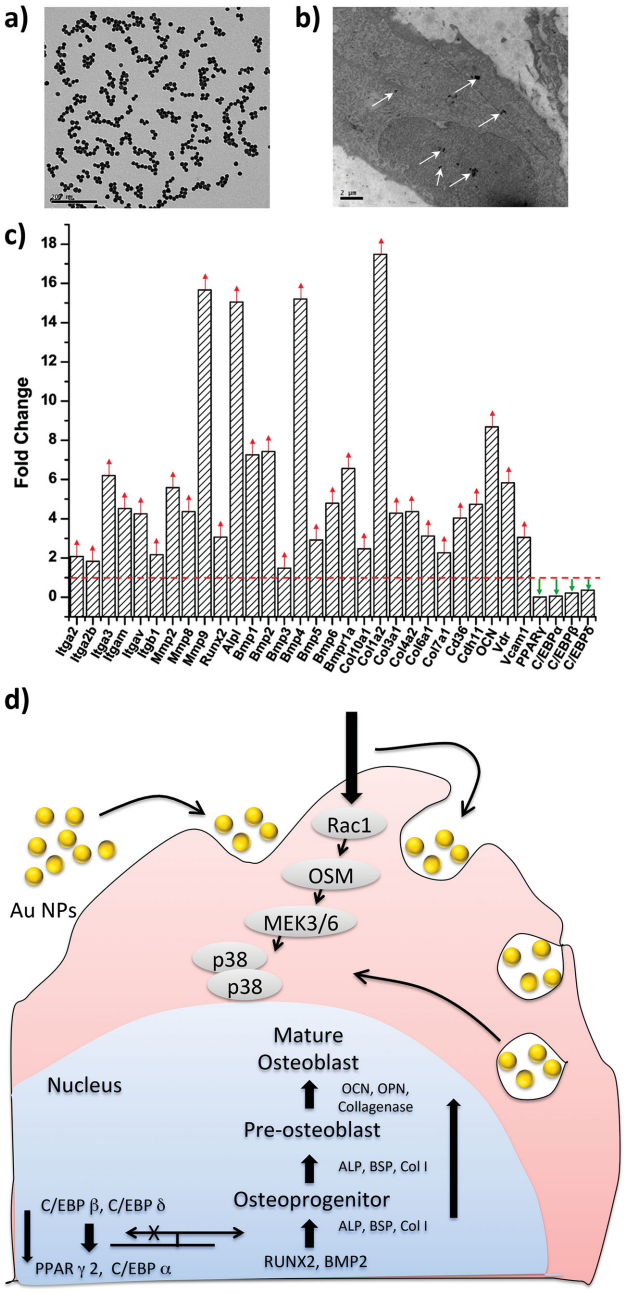

Figure 13. AuNPs-stem cell interactions. a) TEM image show size of Au-nanoparticles ≈21 nm. b) TEM image show internalization of Au nanoparticles inside MSCs as indicated by white arrow. c) Gene analysis indicates upregulation of osteogenic and adipogenic genes due to addition of Au nanoparticles. d) Au nanoparticles modulate osteogenic and adipocytic differentiation of MSCs via p38 MAPK signaling pathway. Reproduced with permission.[125] Copyright 2010, American Chemical Society.

6.3. Superparamagnetic Iron Oxide Nanoparticles

Superparamagnetic iron oxide nanoparticles have been useful in biomedical applications primarily as a MRI contrast agent. As tissue engineering and other stem cell therapies surfaced, SPIONs were proposed as an MRI tracking agent of stem cells. Similar to any other biomaterial, concerns about toxicity can limit the practicality and applicability of their usage. Thus, determining the biological impact of introducing nanomaterials, like SPIONs, to stem cells is crucial. This is especially relevant when the purpose of these particles is to accumulate in a small region, which leads to high localized concentrations and could lead to toxic events.[126] Chen et al. assessed a multitude of osteogenic markers after the application of ferucarbotran, an ionic SPION, and detected dose-dependent inhibition.[127] ALP activity decreased as the concentration increased, and interestingly, MMP2 expression was increased in these cells. This, along with the observation of a decreased proclivity to attach to the substrate, led to the conclusion that osteogenesis was inhibited due to a stimulated propensity for mobilization. Through the

use of an iron chelator, desferrioxamine (DFO), the inhibitory effects of the SPIONs were diminished, illustrating a dependency on free Fe ions to generate a biological response. They suggested that lysosomal degradation of the NPs is responsible for the creation of these ions due to minimal free ion content in the extracellular solution.[127] Other groups have also investigated the potential toxicity of these NPs. The results of these studies have led to a generalized understanding of the particles where cytotoxic levels are fairly high (100 μg/mL) and depend on a variety of parameters like coating, oxidation state of Fe, and protein-particle interactions.[126] Another aspect of SPION–stem cell interactions focuses on cell proliferation. Studies have provided proof of enhanced cellular growth after contact with SPIONs in MSCs. For example, reduced intracellular hydrogen peroxide (H_2O_2) and cell cycle regulatory proteins increased cell cycle progression. Huang et al. noted decreased expression of the tumor suppressor gene p53, decreased expression of $p21^{Cip1}$ and $p27^{Kip1}$ (negative regulators of cell cycle), and AKT activation to avoid apoptosis and aid cell proliferation.[128] Further studies are needed to reveal toxicity mechanisms specific to stem cells and SPIONs.

6.4. Zinc Oxide Nanoparticles

Zinc oxide (ZnO) is another metallic nanomaterial commonly used in a variety of fields that remains poorly understood in terms of biological safety. If its similarity to nanosilver as an antibacterial agent is any indication of its cytotoxicity with mammalian cells, ZnO could have the potential to cause cell death at relatively low concentrations. Therefore, usage of NPs in conjunction with a TE design could be problematic. To better characterize ZnO-NP toxicity, Deng et al. applied four different sizes of particles to NSCs.[129] They found that all sizes showed similar cell viabilities at corresponding concentrations, and a concentration of 12 ppm and above caused significant cell death. They speculated that the lack of dependency on size was due to the formation of similarly sized aggregates for all groups as well as the generation of aqueous Zn ions from the particles. TEM, confocal microscopy, and FACS illustrated the increased activation of apoptosis, which the authors hypothesized stems from mitochondrial inhibition as seen in Zn^{2+} neurotoxicity. Because the NPs were difficult to visualize within the internal structures of the cell, the distinct spatial and temporal event of Zn dissolution was difficult to pinpoint. Thus, the exact mechanism of ZnO toxicity remains unclear. In general, this material seems unsuitable for stem cell therapies, and further caution should be employed in industries that utilize ZnO.[129]

6.5. Titanium Oxide Nanostructures

A development in technology has allowed researchers to modify substrates on the sub-100 nm scale and uncover novel methods to influence cell behavior. Induction of stem cells via changes to the microenvironment through nanotopological structures has become a field of growing interest among researchers in tissue engineering as well as cellular biology. Metal-based nanotube arrays are one such means to modify a substrate and activate specific mechanosensitive pathways to induce differentiation into a targeted cell type. The arrays can utilize a variety of nanotube diameters and spacing to evoke different cellular responses. In one study, the size behavior of TiO_2 nanotube arrays was investigated using MSCs. Researchers found that size effects dominated over surface chemistry of the oxides; there was also an optimal diameter (15 nm) for cell activation. A possibility for this result could stem from the similar length scale of integrin receptors within the membrane (≈10 nm). This enhanced focal contact was also observed in their cellular adhesion experiments, where the greatest cellular density corresponded to nanotube arrays with a diameter of 15 nm.[130]

In a similar study, two anodic currents were applied to fabricate a TiO_2 network with different lateral pore sizes (65 nm and 94 nm).[131] Bauer et al. noted that cell growth was increased on both anodized surfaces; however, the smaller pore network resulted in better growth and showed successful induction of hMSCs into osteogenic cells.[131] The mechanism behind the resulting cellular behavior stems from integrin clustering and activation on the membrane. Why the TiO_2 network has optimized cellular responses at pore sizes greater than the nanotube diameter as well as why 65 nm pores generated a more positive response than the 94 nm pores remains unclear.[131] There is evidence of an optimal length scale for nanotopographies in relation to stem cell behavior, and more specifically, this scale can be modified to induce differentiation into a variety of cell types.

Furthermore, nanotube arrays can be functionalized with relevant proteins to employ a synergistic approach to yield more efficient stem cell differentiation. Multiple studies have proposed enhancing MSC osteogenic differentiation through nanoscale surface geometries integrated with BMP-2.[116,132] The size of the nanotubes again provided important mechanical cues for cellular induction. For an osteogenic response, tubes between 15–30 nm functionalized with BMP-2 showed heightened ALP, OCN, collagen I, and fibronectin expression.[116,133] Interestingly, primary chondrocytes seeded on 100 nm, BMP-2 coated TiO_2 nanotubes maintained their phenotype, while they de-differentiated on 15 nm nanotubes. This finding again indicates the primary role of surface geometry and its influence on cellular induction pathways. It raises the question of an optimal arrangement or geometry to induce differentiation to specific cell types, which has yet to be answered. Lastly, Hu et al. fabricated a TiO_2 nanotube array loaded with BMP-2 and then coated by a multilayer of gelatin/chitosan via a layer-by-layer (LBL) approach.[132] They found that the LBL design increased cell motility as well as the lifetime of BMP-2, leading to significant ALP activity from MSCs. While this approach benefits from the synergistic effects of the gel/chi and BMP-2 as well as from the tunability of drug-loading capacity by varying layer depth, there will be delayed delivery of BMP-2 until the gel/chi layer is degraded, and release of the BMP-2 will be controlled only through passive degradation. The potential of this system will rise with the creation of a smart delivery system to provide a temporally controlled release of the drug.[132]

Metal- and metal-oxide-based nanomaterials have considerable questions regarding cytotoxicity and safety for use with cells. Here we have compiled recent research that has focused on addressing these concerns. While there fails to be a consensus on toxicity for a variety of materials currently in use

commercially and experimentally, some materials are emerging as solutions to a variety of stem cell biology issues. Improved processing and functionalization of these nanomaterials will enable more positive interactions with stem cells, thus making metal and metal oxide nanomaterials more relevant in regenerative medicine applications.

7. Concluding Remarks and Future Challenges

With many nanomaterials, there exists a limited range of bioactivity leading to a positive interaction with target cells. However, this range of bioactivity often exists within a narrow set of limits, and failure to abide within these restrictions proves detrimental to design outcome. One challenge, then, is to improve our evaluation of a nanomaterial's potency to provide a better estimation of a system's potential and refine the design process. Future explorations into potency assays will require an even tighter coupling of material science with molecular and developmental biology. Simultaneously, a continuous challenge exists to enhance stem cell induction via nanomaterial composition. Emerging technologies have enabled fabrication of nanoscale topologies to influence stem cell behavior. Taking a synergistic approach to modifying the stem cell niche by utilizing these technologies in coordination with bioactive nanomaterials and inductive agents could achieve high spatial and temporal control of behavior. Future studies are necessary to determine the amalgamation of cellular pathways for efficacious induction and potency maintenance in conjunction with the timing of activation.

Similar to the evaluation of cell potency, a current challenge exists to properly visualize the interactions of stem cells within this microenvironment. Real-time imaging of cellular function at the sub-micrometer level without altering stem cell behavior or fate will be crucial to pinpointing spatiotemporal mechanisms responsible for induction or cytotoxicity responses. The real time imaging might facilitates the evaluation of the potential of a tissue-engineering construct while concurrently monitoring stem cell behavior in a more relevant environment as opposed to in a culture dish.

Consistent throughout the various types of biomaterials is the interplay between chemical and physical compositions. Interactions with stem cells are due to a combination of material factors (e.g., size, surface chemistry, charge, stiffness) and are highly dependent on cell type and microenvironment. Considerations of these factors prevail within nanomaterial design studies constantly; however, deviations in processing often lead to variations in composition, generating an unexpected cellular response from a seemingly equivalent material. Thus, the observation of nanomaterial interactions in regenerative medicine applications will remain a fundamental design process and will continue to garner interest from the research community as new inductive mechanisms are revealed.

Received: April 14, 2015
Published online: May 26, 2015

[1] a) H. Yang, Y. Xia, *Adv. Mater.* **2007**, *19*, 3085; b) J. Shi, A. R. Votruba, O. C. Farokhzad, R. Langer, *Nano Lett.* **2010**, *10*, 3223; c) A. K. Gaharwar, N. A. Peppas, A. Khademhosseini, *Biotechnol Bioeng.*, **2014**, *111*, 441; d) L. Zhang, T. J. Webster, *Nano Today* **2009**, *4*, 66; e) C. Cha, S. R. Shin, N. Annabi, M. R. Dokmeci, A. Khademhosseini, *ACS Nano* **2013**, *7*, 2891.
[2] V. Mailänder, K. Landfester, *Biomacromolecules* **2009**, *10*, 2379.
[3] Z. Wang, J. Ruan, D. Cui, *Nanoscale Res. Lett.* **2009**, *4*, 593.
[4] F. Zhao, Y. Zhao, Y. Liu, X. Chang, C. Chen, Y. Zhao, *Small* **2011**, *7*, 1322.
[5] Y. Zhang, T. R. Nayak, H. Hongb, W. Cai, *Nanoscale* **2012**, *4*, 3833.
[6] L. Ferreira, *J. Cell. Biochem.* **2009**, *108*, 746.
[7] Y. Xia, *Nat. Mater.* **2008**, *7*, 758.
[8] a) A. Albanese, P. S. Tang, W. C. Chan, *Annual review of biomedical engineering* **2012**, *14*, 1; b) W. H. Suh, Y.-H. Suh, G. D. Stucky, *Nano Today* **2009**, *4*, 27; c) A. C. A. Wan, J. Y. Ying, *Adv. Drug Delivery Rev.* **2010**, *62*, 731; d) E. Martínez, E. Engel, J. A. Planell, J. Samitier, *Ann. Anat.* **2009**, *191*, 126; e) J. K. Carrow, A. K. Gaharwar, *Macromol. Chem. Phys.* **2015**, *216*, 248.
[9] a) P. Bianco, M. Riminucci, S. Gronthos, P. G. Robey, *Stem Cells* **2001**, *19*, 180; b) K. Takahashi, K. Tanabe, M. Ohnuki, M. Narita, T. Ichisaka, K. Tomoda, S. Yamanaka, *Cell* **2007**, *131*, 861; c) M. F. Pittenger, A. M. Mackay, S. C. Beck, R. K. Jaiswal, R. Douglas, J. D. Mosca, M. A. Moorman, D. W. Simonetti, S. Craig, D. R. Marshak, *Science* **1999**, *284*, 143.
[10] a) H. Rippon, A. Bishop, *Cell Proliferation* **2004**, *37*, 23; b) M. Ramalho-Santos, S. Yoon, Y. Matsuzaki, R. C. Mulligan, D. A. Melton, *Science* **2002**, *298*, 597.
[11] I. Ilie, R. Ilie, T. Mocan, D. Bartos, L. Mocan, *Int. J. Nanomed.* **2012**, *2*, 2211.
[12] E. Dawson, G. Mapili, K. Erickson, S. Taqvi, K. Roy, *Adv. Drug Delivery Rev.* **2008**, *60*, 215.
[13] a) A. G. Bang, M. K. Carpenter, *Science* **2008**, *320*, 58; b) M. Tachibana, P. Amato, M. Sparman, N. M. Gutierrez, R. Tippner-Hedges, H. Ma, E. Kang, A. Fulati, H.-S. Lee, H. Sritanaudomchai, K. Masterson, J. Larson, D. Eaton, K. Sadler-Fredd, D. Battaglia, D. Lee, D. Wu, J. Jensen, P. Patton, S. Gokhale, R. L. Stouffer, D. Wolf, S. Mitalipov, *Cell* **2013**, *153*, 1228; c) M. Stadtfeld, K. Hochedlinger, *Gene. Dev.* **2010**, *24*, 2239.
[14] R. Ravichandran, S. Liao, C. C. Ng, C. K. Chan, M. Raghunath, S. Ramakrishna, *World J. Stem Cells* **2009**, *1*, 55.
[15] E. Martínez, A. Lagunas, C. Mills, S. Rodríguez-Seguí, M. Estévez, S. Oberhansl, J. Comelles, J. Samitier, Nanomedicine **2009**, *4*, 65.
[16] L. Ferreira, J. M. Karp, L. Nobre, R. Langer, *Cell Stem Cell* **2008**, *3*, 136.
[17] Kshitiz, D.-H. Kim, D. J. Beebe, A. Levchenko, *Trends Biotechnol.* **2011**, *29*.
[18] a) L. E. McNamara, R. J. McMurray, M. J. P. Biggs, F. Kantawong, R. O. C. Oreffo, M. J. Dalby, *J. Tissue Eng.* **2010**, *1*; b) S. Martino, F. D'Angelo, I. Armentano, J. M. Kenny, A. Orlacchio, *Biotechnol. Adv.* **2012**, *30*, 338.
[19] L. Zhang, T. J. Webster, *Nano Today* **2009**, *4*, 66.
[20] A. K. Gaharwar, S. M. Mihaila, A. Swami, A. Patel, S. Sant, R. L. Reis, A. P. Marques, M. E. Gomes, A. Khademhosseini, *Adv. Mater.* **2013**, *25*, 3329.
[21] a) I. Armentano, M. Dottori, E. Fortunati, S. Mattioli, J. M. Kenny, *Polym. Degrad. Stabil.* **2010**, *95*, 2126; b) L. A. Tran, R. Krishnamurthy, R. Muthupillai, M. d. G. Cabreira-Hansen, J. T. Willerson, E. C. Perin, L. J. Wilson, *Biomaterials* **2010**, *31*, 9482; c) K.-K. Liu, C.-C. Wang, C.-L. Cheng, J.-I. Chao, *Biomaterials* **2010**, *30*, 4249; d) E. L. Bakota, Y. Wang, F. R. Danesh, J. D. Hartgerink, *Biomacromolecules* **2011**, *12*, 1651; e) H. Gul, W. Lu, P. Xu, J. Xing, J. Chen, *Nanotechnology* **2010**, *21*, 155101; f) J. J. Green, B. Y. Zhou, M. M. Mitalipova, C. Beard, R. Langer, R. Jaenisch, D. G. Anderson, *Nano Lett.* **2008**, *8*, 3126.
[22] T.-I. Chao, S. Xiang, C.-S. Chen, W.-C. Chin, A. J. Nelson, C. Wang, J. Lu, *Biochem. Bioph. Res. Co.* **2009**, *384*, 426.

[23] T. Sjöström, M. J. Dalby, A. Hart, R. Tare, R. O. C. Oreffo, B. Sua, *Acta Biomater.* **2009**, *5*, 1433.
[24] K. K. Parker, D. E. Ingber, *Phil. Trans. R. Soc. B* **2007**, *362*, 1267.
[25] N. Wang, J. P. Butler, D. E. Ingber, *Science* **1993**, *260*, 1124.
[26] a) W. Chen, L. G. Villa-Diaz, Y. Sun, S. Weng, J. K. Kim, R. H. Lam, L. Han, R. Fan, P. H. Krebsbach, J. Fu, *ACS Nano* **2012**, *6*, 4094; b) E. K. Yim, E. M. Darling, K. Kulangara, F. Guilak, K. W. Leong, *Biomaterials* **2010**, *31*, 1299; c) B. K. K. Teo, S. T. Wong, C. K. Lim, T. Y. Kung, C. H. Yap, Y. Ramagopal, L. H. Romer, E. K. Yim, *ACS Nano* **2013**, *7*, 4785.
[27] W. J. Li, C. T. Laurencin, E. J. Caterson, R. S. Tuan, F. K. Ko, *J. Biomed. Mater. Res.* **2002**, *60*, 613.
[28] L. E. McNamara, R. J. McMurray, M. J. Biggs, F. Kantawong, R. O. Oreffo, M. J. Dalby, *J. Tissue Eng.* **2010**, *1*, 120623.
[29] A. K. Gaharwar, M. Nikkhah, S. Sant, A. Khademhosseini, *Biofabrication* **2015**, *7*, 015001.
[30] L. Smith, P. Ma, *Colloids Surf. B: Biointerfaces* **2004**, *39*, 125.
[31] D. Li, J. T. McCann, Y. Xia, M. Marquez, *J. Am. Ceramic Soc.* **2006**, *89*, 1861.
[32] a) Y. S. Nam, T. G. Park, *Biomaterials* **1999**, *20*, 1783; b) H. Lo, M. Ponticiello, K. Leong, *Tissue Eng.* **1995**, *1*, 15.
[33] A. Greiner, J. H. Wendorff, *Angew. Chem. Int. Ed.* **2007**, *46*, 5670.
[34] J. Xie, S. M. Willerth, X. Li, M. R. Macewan, A. Rader, S. E. Sakiyama-Elbert, Y. Xia, *Biomaterials* **2009**, *30*, 354.
[35] S. H. Lim, X. Y. Liu, H. Song, K. J. Yarema, H.-Q. Mao, *Biomaterials* **2010**, *31*, 9031.
[36] J. K. Wise, A. L. Yarin, C. M. Megaridis, M. Cho, *Tissue Eng. Pt. A* **2009**, *15*, 913.
[37] N. S. Binulal, M. Deepthy, N. Selvamurugan, K. T. Shalumon, S. Suja, U. Mony, R. Jayakumar, S. V. Nair, *Tissue Eng. Pt. A* **2010**, *16*, 393.
[38] A. S. Nathan, B. M. Baker, N. L. Nerurkar, R. L. Mauck, *Acta Biomater.* **2011**, *7*, 57.
[39] Y. M. Kolambkar, A. Peister, A. K. Ekaputra, D. W. Hutmacher, R. E. Guldberg, *Tissue Eng. Pt. A* **2010**, *16*, 3219.
[40] a) L. A. Smith, X. Liu, J. Hu, P. X. Ma, *Biomaterials* **2010**, *31*, 5526; b) L. A. Smith, X. Liu, J. Hu, P. Wang, P. X. Ma, *Tissue Eng. Pt. A* **2009**, *15*, 1855.
[41] X.-Y. Xu, X.-T. Li, S.-W. Peng, J.-F. Xiao, C. Liu, G. Fang, K. C. Chen, G.-Q. Chen, *Biomaterials* **2010**, *31*, 3967.
[42] M.-H. You, M. K. Kwak, D.-H. Kim, K. Kim, A. Levchenko, D.-Y. Kim, K.-Y. Suh, *Biomacromolecules* **2010**, *11*, 1856.
[43] W. Chen, L. G. Villa-Diaz, Y. Sun, ShinuoWeng, J. K. Kim, R. H. W. Lam, L. Han, R. Fan, P. H. Krebsbach, J. Fu, *ACS Nano* **2012**, *6*, 4094.
[44] M. R. Lee, K. W. Kwon, H. Jung, H. N. Kim, K. Y. Suh, K. Kim, K.-S. Kim, *Biomaterials* **2010**, *31*, 4360.
[45] S. Martino, F. D'Angelo, I. Armentano, R. Tiribuzi, M. Pennacchi, M. Dottori, S. Mattioli, A. Caraffa, G. G. Cerulli, J. M. Kenny, A. Orlacchio, *Tissue Eng. Pt. A* **2009**, *15*, 3139.
[46] K. S. Brammer, C. Choi, C. J. Frandsen, S. Oh, S. Jin, *Acta Biomater.* **2011**, *7*, 683.
[47] a) M. J. Dalby, D. McCloy, M. Robertson, H. Agheli, D. Sutherland, S. Affrossman, R. O. C. Oreffo, *Biomaterials* **2006**, *27*, 1306; b) M. J. Dalby, D. McCloy, M. Roberstson, C. D. Wilkinson, R. O. C. Oreffo, *Biomaterials* **2006**, *27*, 2980.
[48] M. J. Dalby, N. Gadegaard, R. Tare, A. Andar, M. O. Riehle, P. Herzyk, C. D. W. Wilkinson, R. O. C. Oreffo, *Nat. Mater.* **2007**, *6*, 997
[49] J. Y. Lim, A. D. Dreiss, Z. Zhou, J. C. Hansen, C. A. Siedlecki, R. W. Hengstebeck, J. Cheng, N. Winograd, H. J. Donahue, *Biomaterials* **2007**, *28*, 1787.
[50] S. Oh, K. S. Brammer, Y. S. J. Li, D. Teng, A. J. Engler, S. Chien, S. Jin, *Proc. Natl. Am. Soc.* **2009**, *106*, 2130.
[51] R. J. McMurray, N. Gadegaard, P. M. Tsimbouri, K. V. Burgess, L. E. McNamara, R. Tare, K. Murawski, E. Kingham, R. O. C. Oreffo, M. J. Dalby, *Nat. Mater.* **2011**, *10*, 637.
[52] a) M. Rajan, S. Pulavendran, C. Rose, A. B. Mandal, *Int. J. Pharm.* **2011**, *410*, 145; b) S. Zhang, H. Uluda , *Pharm. Res.* **2009**, *26*; c)J. Shi, A. R. Votruba, O. C. Farokhzad, R. Langer, *Nano Lett.* **2010**, *10*, 3223; d) Z. Hongbin, A. Patel, A. K. Gaharwar, S. Mihaila, S. Mukundan, G. Iviglia, H. Bae, H. Yang, A. Khademhosseini, *Biomacromolecules* **2013**, *14*, 1299.
[53] S. Pulavendran, M. Rajam, C. Rose, A. B. Mandal, *IET Nanobiotechnol.* **2010**, *4*, 51.
[54] S. Pulavendran, C. Rose, A. B. Mandal, *J. Nanobiotechnology* **2011**, *9*, 15.
[55] T. Santos, R. Ferreira, J. A. Maia, F. Agasse, S. Xapelli, L. S. Cortes, J. Bragança, J. A. O. Malva, L. Ferreira, L. Bernardino, *ACS Nano* **2012**, *6*, 10463.
[56] J. M. Oliveira, R. A. Sousa, N. Kotobuki, M. Tadokoro, M. Hirose, J. o. F. Mano, R. L. Reis, H. Ohgushi, *Biomaterials* **2009**, *30*, 804.
[57] Z. S. Haidar, F. Azari, R. C. Hamdy, M. Tabrizian, *J. Biomed. Mater. Res. A* **2009**, *91*, 919.
[58] A. Biswas, Y. Liu, T. Liu, G. Fan, Y. Tang, *Biomaterials* **2012**, *33*, 5459.
[59] S. Lorenz, C. P. Hauser, B. Autenrieth, C. K. Weiss, K. Landfester, V. Mailänder, *Macromol. Biosci.* **2010**, *10*, 1034.
[60] L. Florez, C. Herrmann, J. M. Cramer, C. P. Hauser, K. Koynov, K. Landfester, D. Crespy, V. Mailänder, *Small* **2012**, *8*, 2222.
[61] X. Jiang, J. Dausend, M. Hafner, A. Musyanovych, C. Röcker, K. Landfester, V. Mailänder, G. U. Nienhaus, *Biomacromolecules* **2010**, *11*, 748.
[62] a) O. Harush-Frenkela, N. Debottona, S. Benitaa, Y. Altschuler, *Biochem. Bioph. Res. Co.* **2007**, *353*, 26; b) O. Harush-Frenkel, E. Rozentur, S. Benita, Y. Altschuler, *Biomacromolecules* **2008**, *9*, 435.
[63] Y. Zhang, S. Tekobo, Y. Tu, Q. Zhou, X. Jin, S. A. Dergunov, E. Pinkhassik, B. Yan, *ACS Appl. Mater. Inter.* **2012**, *4*, 4099.
[64] R. Agarwal, V. Singh, P. Jurney, L. Shi, S. V. Sreenivasan, K. Roy, *Proc. Natl. Am. Soc.* **2013**, *110*, 17247.
[65] X. G. Cheng, C. Tsao, V. L. Sylvia, D. Cornet, D. Nicolella, T. Bredbenner, R. J. Christy, *Acta Biomater.* **2013**, *10*, 1360.
[66] a) P. Yilgor, K. Tuzlakoglu, R. L. Reis, N. Hasirci, V. Hasirci, *Biomaterials* **2009**, *30*, 3551; b) P. Yilgor, N. Hasirci, V. Hasirci, *J. Biomed. Mater. Res. A* **2010**, *93*, 528.
[67] D. Dyondi, T. J. Webster, R. Banerjee, *Int. J. Nanomed.* **2013**, *8*, 47.
[68] X. Jiang, H. Q. Cao, L. Y. Shi, S. Y. Ng, L. W. Stanton, S. Y. Chew, *Acta Biomater.* **2012**, *8*, 1290.
[69] M. K. Horne, D. R. Nisbet, J. S. Forsythe, C. L. Parish1, *Stem Cells Dev.* **2010**, *19*, 843.
[70] Y. I. Cho, J. S. Choi, S. Y. Jeong, H. S. Yoo, *Acta Biomater.* **2010**, *6*, 4725.
[71] Y. Su, Q. Su, W. Liu, M. Lim, J. R. Venugopal, X. Mo, S. Ramakrishna, S. S. Al-Deyab, M. El-Newehy, *Acta Biomater.* **2012**, *8*, 763.
[72] L. Tian, M. P. Prabhakaran, X. Ding, D. Kai, S. Ramakrishna, *J. Mater. Sci.* **2012**, *47*, 3272.
[73] A. K. Gaharwar, S. M. Mihaila, A. A. Kulkarni, A. Patel, A. D. Luca, R. L. Reis, M. E. Gomes, C. v. Blitterswijk, L. Moroni, A. Khademhosseini, *J. Controlled Release* **2014**, *187*, 66.
[74] J. H. Lee, N. G. Rim, H. S. Jung, H. Shin, *Macromol. Biosci.* **2010**, *10*, 173.
[75] D. Xue, Q. Zheng, C. Zong, Q. Li, H. Li, S. Qian, B. Zhang, L. Yu, Z. Pan1, *J. Biomed. Mater. Res.* **2010**, *94A*, 259.
[76] M. C. Phipps, W. C. Clem, S. A. Catledge, Y. Xu, K. M. Hennessy, V. Thomas, M. J. Jablonsky, S. Chowdhury, A. V. Stanishevsky, Y. K. Vohra, S. L. Bellis, *PLoS One* **2011**, *6*, e16813.

[77] X. Yang, F. Yang, F. Walboomers, Z. Bian, M. Fan, J. A. Jansen, *J. Biomed. Mater. Res.* **2010**, *93A*, 247.
[78] M. Zandi, H. Mirzadeh, C. Mayer, H. Urch, M. B. Eslaminejad, F. Bagheri, H. Mivehchi, *J. Biomed. Mater. Res.* **2009**, *92A*, 1244.
[79] R. Ravichandran, J. R. Venugopal, S. Sundarrajan, S. Mukherjee, S. Ramakrishna, *Biomaterials* **2012**, *33*, 846.
[80] E. Seyedjafari, M. Soleimani, N. Ghaemi, I. Shabani, *Biomacromolecules* **2010**, *11*, 3118.
[81] L. Lin, K. L. Chow, Y. Leng, *J. Biomed. Mater. Res. A* **2009**, *89A*, 326.
[82] H.-C. Liu, L.-L. E, D.-S. Wang, F. Su, X. Wu, Z.-P. Shi, Y. Lv, J.-Z. Wang, *Tissue Eng. Pt. A* **2011**, *17*, 2417.
[83] J. R. Jones, *Acta Biomater.* **2013**, *9*, 4457.
[84] S. Labbaf, O. Tsigkou, K. H. Müller, M. M. Stevens, A. E. Porter, J. R. Jones, *Biomaterials* **2011**, *32*, 1010.
[85] a) J. Mota, N. Yu, S. G. Caridade, G. M. Luz, M. E. Gomes, R. L. Reis, J. A. Jansen, X. F. Walboomers, J. F. Mano, *Acta Biomater.* **2012**, *8*, 4173; b) J. Mota, N. Yu, S. G. Caridade, G. M. Luz, M. E. Gomes, R. L. Reis, J. A. Jansen, X. F. Walboomers, J. F. Mano, *Acta Biomater.* **2012**, *8*, 4173.
[86] S.-J. Hong, H.-S. Yu, K.-T. Noh, S.-A. Oh, H.-W. Kim, *J. Biomater. Appl.* **2010**, *24*, 733.
[87] S. M. Mihaila, A. K. Gaharwar, R. L. Reis, A. Khademhosseini, A. P. Marques, M. E. Gomes, *Biomaterials* **2014**, *35*, 9087.
[88] J. R. Xavier, T. Thakur, P. Desai, M. K. Jaiswal, N. Sears, E. Cosgriff-Hernandez, R. Kaunas, A. K. Gaharwar, *ACS Nano* **2015**, *9*, 3109.
[89] D. Reffitt, N. Ogston, R. Jugdaohsingh, H. Cheung, B. Evans, R. Thompson, J. Powell, G. Hampson, *Bone* **2003**, *32*, 127.
[90] C. A. Gregory, H. Singh, A. S. Perry, D. J. Prockop, *J. Biol. Chem.* **2003**, *278*, 28067.
[91] a) A. K. Gaharwar, V. Kishore, C. Rivera, W. Bullock, C.-J. Wu, O. Akkus, G. Schmidt, *Macromol. Biosci.* **2012**, *12*, 779; b) A. K. Gaharwar, P. J. Schexnailder, B. P. Kline, G. Schmidt, *Acta Biomater.* **2011**, *7*, 568; c) P. J. Schexnailder, A. K. Gaharwar, R. L. Bartlett II, B. L. Seal, G. Schmidt, *Macromol Biosci.* **2010**, *10*, 1416.
[92] S. Wang, R. Castro, X. An, C. Song, Y. Luo, M. Shen, H. Tomas, M. Zhu, X. Shi, *J. Mater. Chem.* **2012**, *22*, 23357.
[93] A. K. Gaharwar, S. Mukundan, E. Karaca, A. Dolatshahi-Pirouz, A. Patel, K. Rangarajan, S. M. Mihaila, G. Iviglia, H. Zhang, A. Khademhosseini, *Tissue Eng. Pt. A* **2014**, *20*, 2088.
[94] G. Nitya, G. T. Nair, U. Mony, K. P. Chennazhi, S. V. Nair, *J. Mater. Sci. Mater. Med.* **2012**, *23*, 1749.
[95] A. J. Mieszawska, J. G. Llamas, C. A. Vaiana, M. P. Kadakia, R. R. Naik, D. L. Kaplan, *Acta Biomater.* **2011**, *7*, 3036.
[96] A. H. Ambre, D. R. Katti, K. S. Katti, *J. Biomed. Mater. Res. A* **2013**, *101A*, 2644.
[97] D. Liu, X. He, K. Wang, C. He, H. Shi, L. Jian, *Bioconjugate Chem.* **2010**, *21*, 1673.
[98] M. V. D. Z. Park, W. Annema, A. Salvati, A. Lesniak, A. Elsaesser, C. Barnes, G. McKerr, C. V. Howard, I. Lynch, K. A. Dawson, A. H. Piersma, W. H. d. Jong, *Toxicol. Appl. Pharm.* **2009**, *240*, 108.
[99] a) D. A. Stout, T. J. Webster, *Mater. Today* **2012**, *15*, 312; b) D. Meng, S. N. Rath, N. Mordan, V. Salih, U. Kneser, A. R. Boccaccini, *J. Biomed. Mater. Res. A* **2011**, *99A*, 435.
[100] T. R. Nayak, L. Jian, L. C. Phua, H. K. Ho, Y. Ren, G. Pastorin, *ACS Nano* **2010**, *4*, 7717.
[101] D. Liu, C. Yi, D. Zhang, J. Zhang, M. Yang, *ACS Nano* **2010**, *4*, 2185.
[102] C. Y. Tay, H. Gu, W. S. Leong, H. Yu, H. Q. Li, B. C. Heng, H. Tantang, S. C. J. Loo, L. J. Li, L. P. Tan, *Carbon* **2010**, *48*, 1095
[103] N. W. S. Kam, E. Jan, N. A. Kotov, *Nano Lett.* **2009**, *9*, 273.
[104] A. M. Schrand, J. Johnson, L. Dai, Saber M. Hussain, J. J. Schlager, L. Zhu, Y. Hong, E. O. Sawa, in *Safety of Nanoparticles*, Springer, New York **2009**.
[105] H. K. Lindberg, G. C.-M. Falck, S. Suhonen, M. Vippola, E. Vanhala, J. Catalán, K. Savolainen, H. Norppa, *Toxicol. Lett.* **2009**, *186*, 166.
[106] W. C. Lee, C. H. Y. X. Lim, H. Shi, L. A. L. Tang, Y. Wang, C. T. Lim, K. P. Loh, *ACS Nano* **2011**, *5*, 7334.
[107] T. R. Nayak, H. Andersen, V. S. Makam, C. Khaw, S. Bae, X. Xu, P.-L. R. Ee, O.-H. Ahn, B. H. Hong, G. Pastorin, B. Ozyilmaz, *ACS Nano* **2011**, *5*, 4670.
[108] S. Y. Park, J. Park, S. H. Sim, M. G. Sung, K. S. Kim, B. H. Hong, S. Hong, *Adv. Mater.* **2011**, *23*, H263.
[109] G.-Y. Chen, D. W.-P. Pang, S.-M. Hwang, H.-Y. Tuan, Y.-C. Hua, *Biomaterials* **2012**, *33*, 418.
[110] R. Tatavarty, H. Ding, G. Lu, R. J. Taylor, X. Bi, *Chem. Commun.* **2014**, *50*, 8484.
[111] a) M. Yang, J. Yao, Y. Duan, *The Analyst* **2013**, *138*, 72; b) M. Gu, Y. Liu, T. Chen, F. Du, X. Zhao, C. Xiong, Y. Zhou, *Tissue Eng. Part B: Rev.* **2014**, *20*, 477.
[112] O. Akhavan, E. Ghaderi, H. Emamy, F. Akhavan, *Carbon* **2013**, *54*, 419.
[113] A. Sasidharan, L. S. Panchakarla, P. Chandran, D. Menon, S. Nair, C. N. R. Rao, M. Koyakutty, *Nanoscale* **2011**, *3*, 2461.
[114] O. Akhavan, E. Ghaderi, A. Akhavan, *Biomaterials* **2012**, *33*, 8017.
[115] Y. Xing, W. Xiong, L. Zhu, E. Osawa, S. Hussin, L. Dai, *ACS Nano* **2011**, *5*, 2376.
[116] J. Park, S. Bauer, A. Pittrof, M. S. Killian, P. Schmuki, K. von der Mark, *Small* **2012**, *8*, 98.
[117] C. Greulich, S. Kittler, M. Epple, G. Muhr, M. Koller, *Langenbeck. Arch. Surg.* **2009**, *394*, 495.
[118] S. Kittler, C. Greulich, M. Koller, M. Epple, *Materialwiss. Werkst.* **2009**, *40*, 258.
[119] C. Greulich, J. Diendorf, T. Simon, G. Eggeler, M. Epple, M. Koller, *Acta Biomater.* **2011**, *7*, 347.
[120] S. Hackenberg, A. Scherzed, M. Kessler, S. Hummel, A. Technau, K. Froelich, C. Ginzkey, C. Koehler, R. Hagen, N. Kleinsasser, *Toxicol. Lett.* **2011**, *201*, 27.
[121] P. V. AshaRani, G. L. K. Mun, M. P. Hande, S. Valiyaveettil, *ACS Nano* **2009**, *3*, 279.
[122] M. V. D. Z. Park, A. M. Neigh, J. P. Vermeulen, L. J. J. de la Fonteyne, H. W. Verharen, J. J. Briede, H. van Loveren, W. H. de Jong, *Biomaterials* **2011**, *32*, 9810.
[123] M. E. Samberg, E. G. Loboa, S. J. Oldenburg, N. A. Monteiro-Riviere, *Nanomedicine* **2012**, *7*, 1197.
[124] D. G. Woo, M. S. Shim, J. S. Park, H. N. Yang, D. R. Lee, K. H. Park, *Biomaterials* **2009**, *30*, 5631.
[125] C. Q. Yi, D. D. Liu, C. C. Fong, J. C. Zhang, M. S. Yang, *ACS Nano* **2010**, *4*, 6439.
[126] N. Singh, G. J. Jenkins, R. Asadi, S. H. Doak, *Nano Rev.* **2010**, *1*.
[127] Y. C. Chen, J. K. Hsiao, H. M. Liu, I. Y. Lai, M. Yao, S. C. Hsu, B. S. Ko, Y. C. Chen, C. S. Yang, D. M. Huang, *Toxicol. Appl. Pharm.* **2010**, *245*, 272.
[128] D. M. Huang, J. K. Hsiao, Y. C. Chen, L. Y. Chien, M. Yao, Y. K. Chen, B. S. Ko, S. C. Hsu, L. A. Tai, H. Y. Cheng, S. W. Wang, C. S. Yang, Y. C. Chen, *Biomaterials* **2009**, *30*, 3645.
[129] X. Y. Deng, Q. X. Luan, W. T. Chen, Y. L. Wang, M. H. Wu, H. J. Zhang, Z. Jiao, *Nanotechnology* **2009**, *20*.
[130] S. Bauer, J. Park, J. Faltenbacher, S. Berger, K. von der Mark, P. Schmuki, *Integr. Biol.* **2009**, *1*, 525.
[131] C. Y. Chiang, S. H. Chiou, W. E. Yang, M. L. Hsu, M. C. Yung, M. L. Tsai, L. K. Chen, H. H. Huang, *Dent. Mater.* **2009**, *25*, 1022.
[132] Y. Hu, K. Cai, Z. Luo, D. Xu, D. Xie, Y. Huang, W. Yang, P. Liu, *Acta Biomater.* **2012**, *8*, 439.
[133] M. Lai, K. Cai, L. Zhao, X. Chen, Y. Hou, Z. Yang, *Biomacromolecules* **2011**, *12*, 1097.

